Li *et al. Energy Mater.* **2025**, *5*, 500069
DOI: 10.20517/energymater.2024.236

Energy Materials

Review

Open Access

Check for updates

Electrospun fiber-based electrodes materials for flexible lithium-ion batteries

Zijian Li[1,#], Mingyang Li[2,#], Wanyu He[1,#], Bin Fei[1,*]

[1]School of Fashion and Textiles, The Hong Kong Polytechnic University, Kowloon 999077, Hong Kong, China.
[2]Centre for Ionics Universiti Malaya, Universiti Malaya, Kuala Lumpur 50603, Malaysia.
[#]Authors contributed equally.

***Correspondence to:** Prof. Bin Fei, School of Fashion and Textiles, The Hong Kong Polytechnic University, Hung Hom Road, Kowloon 999077, Hong Kong, China. E-mail: bin.fei@polyu.edu.hk

How to cite this article: Li, Z.; Li, M.; He, W.; Fei, B. Electrospun fiber-based electrodes materials for flexible lithium-ion batteries. *Energy Mater.* **2025**, *5*, 500069. https://dx.doi.org/10.20517/energymater.2024.236

Received: 30 Oct 2024 **First Decision:** 30 Nov 2024 **Revised:** 6 Dec 2024 **Accepted:** 10 Dec 2024 **Published:** 10 Mar 2025

Academic Editor: Bin Wang **Copy Editor:** Fangling Lan **Production Editor:** Fangling Lan

Abstract

Flexible lithium-ion batteries (FLBs) hold a promising future in the fields of wearable electronic accessories, wearable therapeutic devices, *etc*. due to their long cycle life, good flexibility, and the transferable experience from traditional rigid lithium-ion batteries. Additionally, electrospinning technology, as an important method of synthesizing fiber materials, has good controllability and shows incomparable advantages in the preparation of fiber-based electrodes. Therefore, this review first discusses the assessment of flexibility and proposes that standardized assessment methods are the foundation for the development of flexible energy storage devices. It then analyzes in detail the principle of electrospinning technology and the impact of various parameters on electrode performance, exploring the controlling of the morphology of fibers by optimizing process parameters. The pivotal role of electrospinning technology in manufacturing FLBs is also discussed, with a particular focus on its contribution to enhancing energy density, cycling stability, and mechanical flexibility in both cathode and anode materials. Overall, the review provides guidance for the development of high-performance FLBs.

Keywords: Flexible lithium-ion batteries, electrospinning technology, fiber-based electrodes, flexibility assessment

INTRODUCTION

With the increasing attention and demand for wearable electronic devices, the market for flexible electronic technology has fully developed globally. In 2023, the global wearable technology market generated an

impressive revenue of $71.915 billion [Figure 1A][1]. As major companies, including Huawei Technologies, Nike Inc., and Samsung Electronics Co Ltd., continue to enter the market, and as advanced wearable devices, such as virtual reality glasses and blood oxygen monitoring wristbands, evolve, the industry is poised for rapid growth. From 2024 to 2030, headwear and eyewear are projected to become the second largest and second fastest-growing product areas after wrist-worn wearable electronic devices. By 2030, the global wearable technology market is expected to reach an unprecedented $186.1428 billion[2].

In order to ensure a secure and comfortable fit, flexibility has become an indispensable attribute of wearable electronic devices. Traditional rigid batteries are unable to guarantee the normal operation of electronic devices under specific conditions such as bending, twisting, and folding. When exposed to external forces, they may, at a minimum, experience detachment of electrode materials leading to the electrical failure of active substances or, at a maximum, induce leakage of toxic electrolytes, puncture the separator, and even cause combustion and explosions due to short circuits[3]. Consequently, rigid batteries significantly restrict the conformal contact of wearable electronic devices with the human body, and their safety concerns also impede the advancement of wearable electronics. In contrast to rigid batteries, flexible batteries not only maintain the fundamental function of powering flexible electronic devices but are also capable of adapting to their shape design and enduring repeated twisting conditions[4]. Hence, flexible batteries provide a broader range of possibilities for wearable electronic devices.

Flexible batteries, in addition to showing considerable potential in consumer wearable electronic devices such as wristwatches and virtual reality glasses, also exhibit significant advantages in numerous fields including healthcare, smart textiles, and electric vehicles. For instance, due to their high flexibility and moldability, these batteries play an important role in implantable medical devices, capable of conforming to the movement and tissue deformation of the human body to achieve the appropriate shape[5]. Lithium-ion batteries (LIBs), with their high specific capacity and long cycle life, have dominated the majority of the energy storage market. Owing to their mature manufacturing processes and comprehensive industrial chains, LIBs have experience and a foundation for exploration in the field of flexibility. For example, all-hydrogel tissue-like flexible LIBs have achieved a capacity of 82 mAh g^{-1} at 0.5 A g^{-1}[6]. Their Young's modulus of 80 kPa perfectly matches the mechanical properties of biological tissues, demonstrating excellent performance in wearable and implantable applications [Figure 1B]. Furthermore, Lu *et al.* have made cutting-edge explorations about smart textiles[7], rotating multiple anode and cathode fibers and separators, with the electrolyte solution permeating and polymerizing through the aligned channels formed by these components, achieving an intimate and stable interface between the gel electrolyte and the electrodes [Figure 1C]. Flexible lithium batteries (FLBs) based on $LiCoO_2$ (LCO) and graphite maintain a good discharge capacity of 170 mAh g^{-1} as the number of wound fibers increases from 4 to 8, and exhibit a cycle stability of 87.7% after 1,000 cycles. High-performance fiber-type FLBs can be mass-produced on a scale of hundreds to thousands of meters and perform excellently in fire-resistant fabrics. Firefighting suits constructed with these FLBs can maintain a stable voltage of around 4.35 V even when heated to above 80 °C [Figure 1D]. Moreover, when the firefighting suits are discharged at a constant current rate of 1C, they can withstand extreme conditions such as twisting, hammering, cutting, and boiling water without failure, instead achieving stable discharge. Additionally, this FLB demonstrates application value in the aerospace field. Specifically, the FLB fabric can stably power the solar panels in a vacuum at -0.08 MPa, and will not experience electrolyte leakage or battery failure even when cut. Furthermore, under ultraviolet light and at temperatures as low as -40 °C, the FLB fabric can also stably discharge and power solar panels.

In the development of FLBs, fiber-based materials have shown great potential as cathode and anode materials for FLBs due to their unique 1D structural characteristics and mechanical flexibility[8]. Specifically,

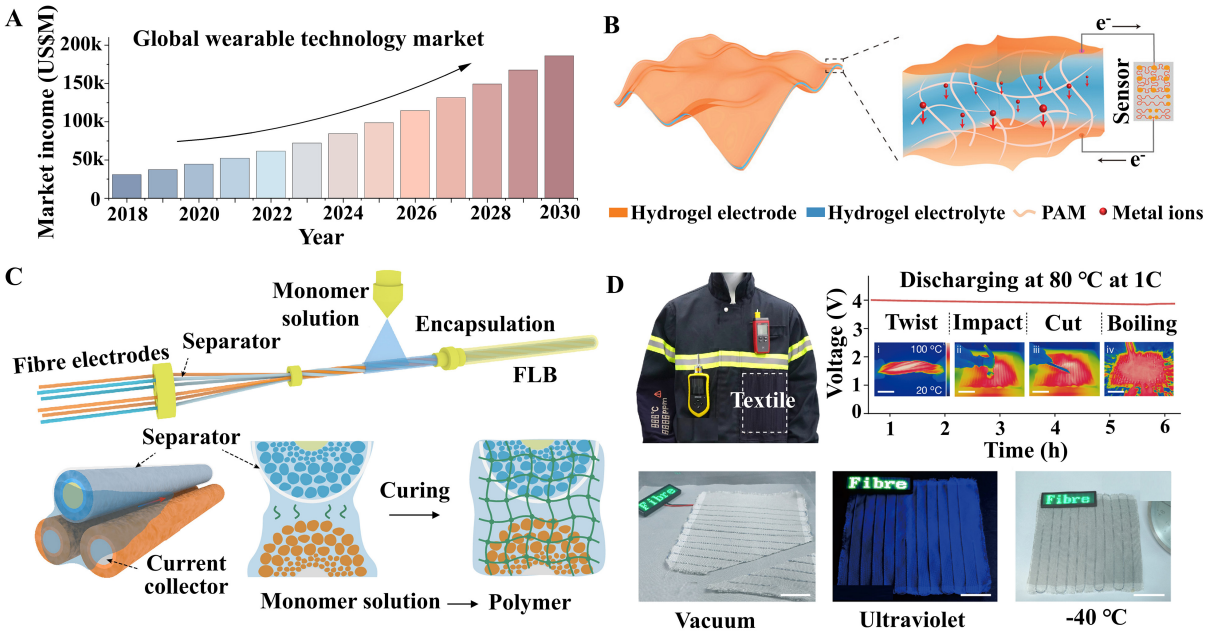

Figure 1. (A) The market income forecast based on the existing global wearable technology market[1]. (B) The all-hydrogel tissue-like flexible LIBs used in wearable and implantable applications[6]. Copyright 2021, Wiley. (C) Fiber-type FLBs based on the design of gel electrolyte. (D) Textiles based on fiber-type FLBs maintain excellent performance under various harsh conditions[7]. Copyright 2024, Springer Nature.

the high specific surface area of 1D fiber-based materials provides more reaction sites for active materials, which helps enhance the specific capacity. The flexibility of fiber-based materials allows them to adapt to various battery shapes and sizes, meeting the needs of wearable devices and flexible electronics. Electrospinning technology, as an efficient and cost-effective method, is often used to prepare fiber materials with diameters ranging from nanometers to micrometers. This technique involves applying a high voltage to eject a fine thread of polymer solution along with electrode particles or electrode precursors, with the solvent evaporating during flight, ultimately forming a fiber deposit on the collector.

Electrospinning technology has shown significant advantages in the preparation of fiber electrodes, including high specific surface area, structural controllability, compositional diversity, mechanical flexibility, and high porosity[9]. Therefore, in recent years, this technology has been proven to be crucial for the design of electrodes for flexible energy storage devices (FESDs)[10]. It is worth noting that electrospinning is expected to change the brittleness and high sensitivity to defects of traditional oxides[11]. For instance, SiO_2 nanowires prepared by electrospinning without the addition of polymers have a tensile strength of up to 1.41 GPa and a toughness of up to 34.29 MJ m^{-3}[12]. SiO_2, as an important anode material, has a high energy density[13]; thus, this discovery greatly promotes the realization of flexible inorganic anode fibers. Furthermore, electrospinning technology helps to achieve large-scale production of electrode materials[14], such as $TiNb_2O_7$ anode materials with unique pre-distorted $Nb(Ti)O_6$ octahedra that can be produced on a large scale with a length of up to 3 m under high charging/discharging rates, showing stability and high capacity[15]. These materials possess high flexibility and mechanical strength, and they have great application value and potential for expansion in FESDs, highlighting the key role of electrospinning technology in preparing high-power-density FESDs. In addition, flexible metal fabrics based on nickel-cotton prepared by electrospinning have ultra-high bending stability and high areal capacitance (973.5 mF cm^{-2}), which is of great significance for wearable supercapacitors[16]. Moreover, electrospinning technology has unique advantages in integration and integration. Due to its continuous manufacturing characteristics[17], it is

possible to sequentially spin the cathode, polymer solid electrolyte, and anode by changing the pre-electrospinning solution to prepare an all-in-one battery and other energy storage devices[18]. Moreover, its continuous manufacturing characteristics also allow the battery to be combined with other multifunctional electronic devices, such as the integration with lighting, data transmission, and biochemical sensing fibers, to obtain multifunctional electronic devices[19,20]. Therefore, electrospinning technology plays a key role in the design of flexible battery electrodes. By precisely controlling the morphology and structure of the fibers, electrospinning technology can produce fiber electrodes that have excellent electrochemical performance and high flexibility[21]. With further research and optimization of electrospinning technology, it is expected that FLBs will play an increasingly important role in future flexible electronic devices.

Therefore, this review focuses on the application of cathodes and anodes prepared by electrospinning technology in FLBs, and specifically summarizes the methods of incorporating cathode materials through electrospinning technology, where in some studies, researchers directly incorporate cathode active materials into the pre-spinning solution to obtain fiber-based cathodes through electrospinning. Additionally, some researchers add precursors of cathode materials to the pre-spinning solution and conduct post-treatment methods after electrospinning to achieve the synthesis of flexible cathodes. Notably, self-supported cathodes, which can significantly reduce the mass of inactive substances, can be realized through electrospinning and hold great promise. Moreover, for anodes, different lithium storage mechanisms determine that anodes have different theoretical capacities and degradation mechanisms. Electrospinning technology can often incorporate different doping elements or substances into the pre-spinning solution to improve properties such as conductivity. Furthermore, organic precursors in the pre-spinning solution can form a three-dimensional (3D) conductive network after electrospinning and subsequent carbonization, providing a buffer for the volume changes of alloy-type anodes and conversion-type anodes. This review assesses the impact of electrospinning technology on the performance enhancement of electrodes, focusing on the optimization of process parameters to achieve higher energy density, better cycling stability, and improved mechanical flexibility. It serves as a significant reference for the design and manufacturing of next-generation high-performance FESDs.

THE ASSESSMENT OF THE FLEXIBILITY OF FLBS

The assessment of the "flexibility" of FLBs is a crucial criterion that distinguishes FLBs from traditional rigid LIBs. Appropriate evaluation methods are the essential theoretical foundation for establishing industry standards for FLBs and a necessary prerequisite for the large-scale commercialization of FLBs. Testing for flexibility belongs to mechanical property testing, primarily aimed at determining the extent to which batteries can withstand deformations caused by external forces while still operating normally, or the durability of batteries that can repeatedly deform under repeated external forces and continue to function properly[22]. Due to external forces, FLBs may undergo deformation in various forms, such as bending, folding, and stretching. Under such test conditions, FLBs must maintain stable charging and discharging properties without significant impact to ensure reliable performance in everyday activities, such as sports and washing. For FESDs, the bending angle (θ), curvature radius (R), and device length (L) are important parameters influencing mechanical deformation. As shown in Figure 2A[23], the longer the L, the smaller the proportion of the stressed area volume to the total device volume, but L does not affect the local stress experienced by the force. In contrast, θ and R are the key factors influencing local stress. Specifically, a larger θ and a smaller R can generate greater local stress. If FLBs can maintain good electrochemical performance under these conditions, their good flexibility is demonstrated.

Due to the diverse assessment methods currently employed in research, sometimes even manual application of external forces is used, making it difficult to compare and measure FLBs by the same standards.

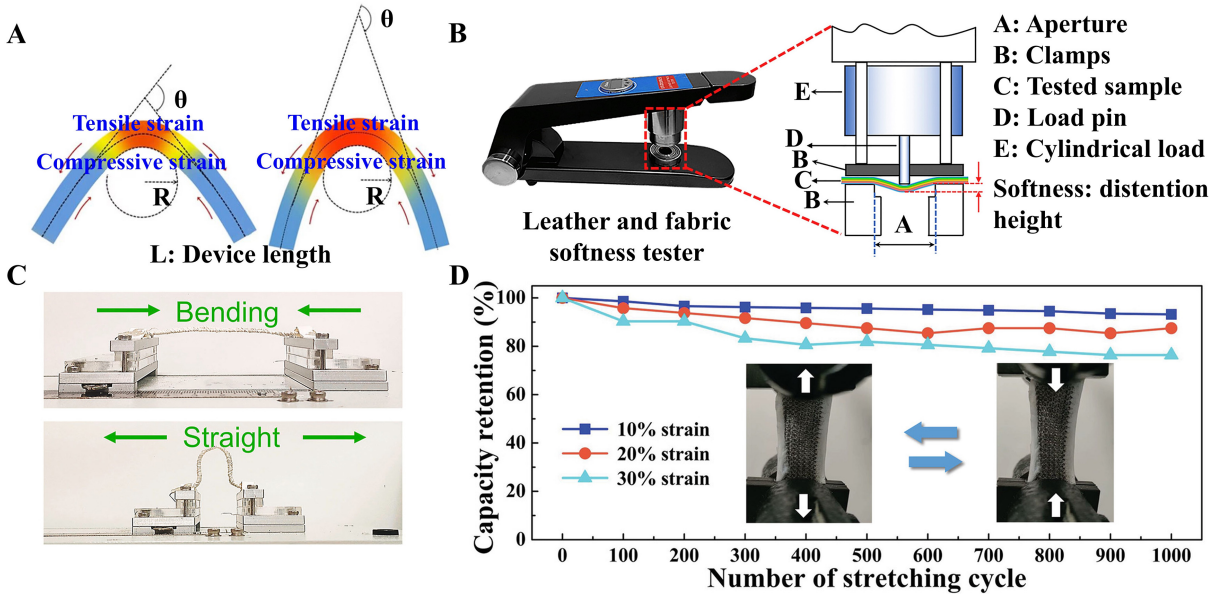

Figure 2. (A) The influence of different bending angles θ and curvature radius R on compressive strain in flexible devices. (B) The flexibility tests conducted by commercial leather and fabric softness testers[23]. Copyright 2019, Elsevier. (C) Quantify strain through clamp measurement[24]. Copyright 2023, Elsevier. (D) Electrochemical measurement with different stretching ratios controlled by clamps[25]. Copyright 2020, Wiley.

Therefore, the development of characterization equipment plays a significant role in promoting the flexibility assessment. Inspired by the similarity between the gel electrolyte and packaging of FESDs and leather, Li *et al.* refer to the softness testing methods of the leather and textile industry. They use a commercial leather and fabric softness tester to perform flexibility tests on FESDs [Figure 2B][23]. Specifically, by clamping the tested sample (FESDs) between two clamps and securing it, an external force is applied to the load pin through a cylindrical load. The load pin approaches and contacts the FESDs at a specified rate without causing device failure. The maximum distension height reached under these conditions can be considered as its softness, and this method can be used to quantitatively assess the flexibility of FESDs.

Additionally, a simple clamp can fix the ends of FESDs, and the stress can be adjusted by changing the distance between the clamps. Unlike the external forces manipulated by hand, the control of external forces achieved through the clamp allows for the quantification of the degree of strain. The control of external forces through the clamp is applied in both fiber- [Figure 2C][24] and thin-film-type FESDs [Figure 2B]. Notably, this testing method can be combined with electrochemical testing, allowing FESDs to deform while charging and discharging. By analyzing voltage curves or long-term capacity retention of the batteries, a better assessment of their comprehensive performance can be achieved. For instance, a stretchable flexible capacitor underwent galvanostatic charge-discharge (GCD) testing at 8 A g^{-1} during stretch-release experiments [Figure 2D][25]. After 1,000 stretch-release cycles at strains of 10%, 20%, and 30%, the capacity decreased only by 6.8%, 12.5%, and 23.6%, respectively, confirming its high stretchability and stable electrochemical cycling performance.

In summary, manually bending or stretching FLBs without causing power interruption is unreliable for assessing their flexibility. The development of standardized flexible testing devices is essential for effectively evaluating the flexibility of FLBs.

ELECTROSPINNING TECHNOLOGY

Electrospinning technology, proposed in the early 20th century, has been widely used in nanotechnology and materials science for mass production of high-quality nanofibers due to its low cost, simple operation, and relatively modest equipment requirements[26]. Although its production capacity may be lower than that of traditional methods such as hydrothermal and combustion synthesis, electrospinning offers the advantage of precise control over fiber diameter and structure. This capability is crucial for synthesizing specific nanostructures that are difficult to achieve with other methods. Especially for FESDs, electrospinning technology is used to prepare nanofiber electrode materials. These fibers, with their high specific surface area, good electrical conductivity, and excellent mechanical properties, greatly enhance the capacity and cycle life of batteries. The following discussion will explore the principle of electrospinning technology and the impact of parameter optimization on the physicochemical properties and electrochemical performance of fibers.

Principle

The basic working principle of electrospinning technology is to apply an electric force to a polymer solution using a high-voltage electric field, causing the solution to be stretched into nanoscale fibers from the nozzle under the influence of the electric field[27]. The entire spinning process can be divided into four parts: Droplet formation; Taylor cone and jet formation; Jet stretching and solidification; and Fiber collection.

Electrospinning begins with the formation of a droplet at the nozzle [Figure 3A]. The pre-spinning solution is extruded through a syringe pump under an electric field, and the droplet maintains a circular shape due to surface tension[28]. However, when the applied voltage increases to a certain extent, the electrostatic force begins to act on the droplet, causing it to deform. As the electric field force increases, when the electrostatic force exceeds the surface tension, the droplet begins to sharpen, which is a prelude to the formation of the Taylor cone[29]. Taylor derived the voltage balance equation for the Taylor cone and calculated that the angle of a stable Taylor cone is 49.3°, and this result was experimentally verified in 1969[30]. When the voltage rises to the critical value, the surface tension of the droplet is broken by the electrostatic force, forming a Taylor cone. The closer the voltage is to the critical value, the more stable the formed Taylor cone is, and the uniformity of the jet is also higher. When the applied electric field reaches a sufficient intensity, the polymer jet is ejected from the tip of the Taylor cone, and this jet is immediately further acted upon by the electrostatic force and stretched, with the diameter of the fiber gradually decreasing as the jet is stretched. During the stretching process, the solvent evaporates or the polymer solidifies, and the fiber gradually solidifies. After forming the fibers, they are usually collected by a collector (such as a conductive flat plate or rotating drum)[31]. The type and operation mode of the collector will affect the arrangement and final structure of the fibers. For example, using a high-speed rotating drum can obtain orderly arranged fibers, thus forming a fiber membrane with directionality.

Parameters

Optimizing the electrospinning process can control the diameter, morphology, and structure of fibers to meet various application requirements. Process optimization includes adjusting several parameters such as electric field strength, solution properties, nozzle diameter, spinning distance, and the speed of the collection roller.

Electric field intensity

Electric field intensity is one of the core parameters that determine the morphology of fibers. The greater the electric field intensity, the stronger the stretching force on the polymer jet, resulting in finer fibers[32]. Typically, an increase in voltage can significantly reduce the diameter of fibers[33]. For example, Figure 3B

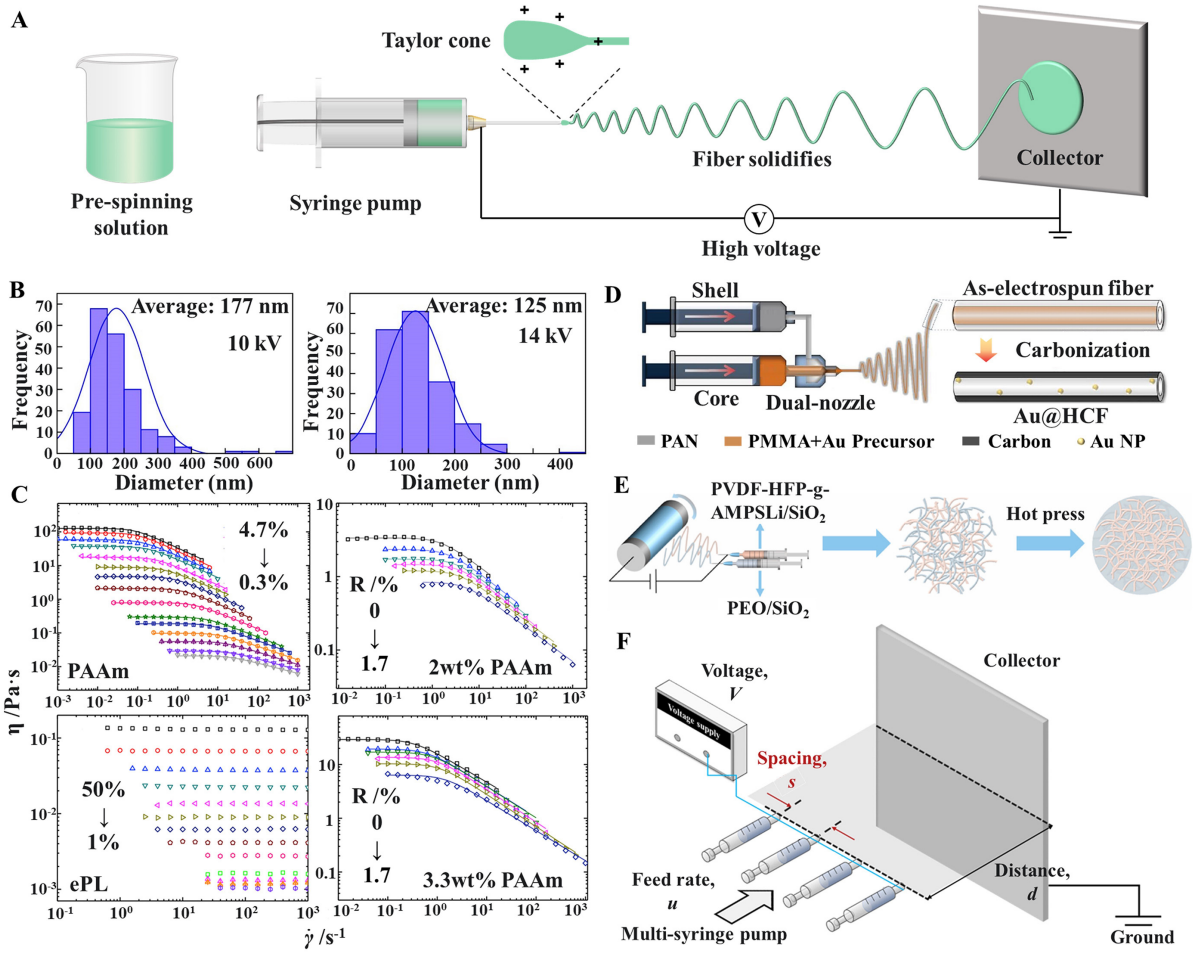

Figure 3. (A) The schematic diagram of electrospinning process. (B) Fiber diameter distribution under different electrospinning voltages[34]. Copyright 2024, Wiley. (C) The viscosity comparison of pre-spinning solutions with different molecular weights[36]. Copyright 2020, Elsevier. (D) The core-shell structured nanofibers prepared by dual-nozzle design[43]. Copyright 2021, Elsevier. (E) The control of relative content of lithium salts and PEO in solid electrolytes by adjusting the number of nozzles[44]. Copyright 2021, Elsevier. (F) Schematic diagram exploring the influence of electrospinning distance on fibers based on multi-nozzle system[46]. Copyright 2023, Wiley.

compares the fiber diameter of poly(vinylidene fluoride-co-hexafluoropropylene) (PVDF-HFP)-based separators for LIBs under different voltages[34], demonstrating that an increase in voltage leads to a decrease in fiber diameter. However, an overly strong electric field can also cause the Taylor cone to not form completely, resulting in jet instability, which can lead to the jet splitting or forming beaded structures. Therefore, the optimization of electric field intensity should be controlled within a certain range.

Solution properties

The viscosity, concentration, and surface tension of polymer solutions are critical factors in fiber formation. High-viscosity solutions typically produce thicker fibers, while low-viscosity solutions tend to yield finer fibers[35]. Solution viscosity depends on the molecular weight of the polymer and the properties of the solvent. High molecular weight polymers provide a stronger entanglement force of molecular chains, which can resist jet breakage, thereby forming a stable fiber structure. For example, ultra-high molecular weight polyacrylamide (PAAm) and low molecular weight ε-polylysine (ePL), when used alone for electrospinning, both have viscosities that are difficult to meet the requirements for defect-free fiber formation

[Figure 3C][36]. However, in the PAAm-ePL mixed solution, viscosity is primarily governed by PAAm [Figure 3]. The addition of ePL significantly reduces the solution viscosity, ultimately enabling the production of defect-free fibers.

Furthermore, the evaporation rate of the solvent significantly influences fiber formation. If the solvent evaporates too quickly, it can cause the fibers to solidify prematurely, limiting the stretching of the fibers and resulting in thicker fibers; if it evaporates too slowly, it may lead to surface adhesion of the fibers or the formation of irregular structures[37]. In studies exploring the impact of the addition of low boiling point solvent tetrahydrofuran (THF) on the performance of separators for LIBs[38], researchers found that the acceleration of solvent evaporation reduces the adhesion between fibers, which is beneficial for providing better tensile strain performance (approximately 36.9%).

It is important to note that the conductivity of the solution also affects the spinning process. Moderate conductivity helps to increase the stability of the jet and the uniformity of the fibers. For example, ionic liquids (ILs), which are materials with high ionic conductivity, can significantly improve the conductivity and surface tension of the spinning solution[39]. These properties are beneficial for constructing a porous structure with abundant mesopores in Sn-C anodes[40], buffering the volume change of Sn particles, and achieving a reversible capacity of 750 mAh g^{-1} at 0.5 A g^{-1}.

Nozzle structure

The design and diameter of the nozzle directly affect the shape and flow rate of the polymer solution being ejected, thereby determining the morphology and diameter of the fibers[41]. A smaller nozzle diameter typically results in finer fibers because the reduced liquid flow rate decreases the likelihood of forming thick fibers. However, an excessively small nozzle diameter may lead to jet instability or even clogging of the nozzle. Precise control of the nozzle diameter can achieve a stable jet and uniform fiber diameter.

Moreover, the design of the nozzle structure is crucial for achieving high-performance LIBs[42]. For instance, a dual-nozzle design can create core-shell structured nanofibers. By using a dual-nozzle design, gold nanoparticles can be embedded within carbon nanowires [Figure 3D][43], regulating the uniform deposition of lithium and achieving reversible cycling. Additionally, solid electrolytes prepared by multi-nozzle electrospinning technology and hot-pressing method [Figure 3E] can control the relative content of lithium salts and poly (ethylene oxide) (PEO) in the solid electrolyte by adjusting the number of nozzles, thereby affecting the Li^+ transport efficiency[44]. Achieving large-scale production of solid electrolytes by simply adjusting the nozzle structure is of great significance for the development of FLBs.

Spinning distance

Spinning distance, the distance between the nozzle and the collector, is an important parameter affecting fiber formation. An appropriate spinning distance ensures sufficient stretching of the polymer jet and effective solvent evaporation, resulting in a uniform fiber structure[45]. A spinning distance that is too short may lead to fiber adhesion or incomplete curing, while an excessively long distance may cause over-stretching or even breakage. For example, in studies exploring the effect of spinneret-to-collector distance on gelatin-based electrospun fibers using a multi-nozzle system and keeping other parameters constant [Figure 3F][46], as the distance increases from 10 to 12 cm and then to 14 cm, two effects were observed. On the one hand, greater stretching occurs at a longer spinning distance, and on the other hand, the electric field strength between the nozzle and the collector decreases, further reducing the stretching force on the nanofibers. These combined effects contributed to an increase in the diameter of the nanofibers.

Collection substrate and collection roller speed

A metal flat plate, as a traditional conductive collection substrate, has a lower cost, but the morphology and structure of the prepared nanofibers are difficult to control precisely[47]. Therefore, the commonly used collection substrate at present is the rotating drum, which, in a rapidly rotating state, can produce highly oriented and uniform nanofibers[48]. During the electrospinning process, the speed of the collection roller significantly affects the arrangement and structure of the fibers. For example, as the rotation speed increases from 700 to 2,100 rpm, the average diameter of the manufactured fibers shows a clear downward trend (from 850 ± 25 nm to 298 ± 20 nm)[49], which is considered to be related to the stretching and extension of the polymer jet. A higher rotation speed can align fibers in an orderly manner, making them suitable for applications requiring enhanced mechanical properties, such as high-strength composite materials.

Additionally, it is worth noting that coaxial electrospinning can produce structures with multiple polymer layers, which can combine various excellent properties[50]. For example, the fire-resistant core-shell battery separator synthesized by the coaxial electrospinning technique has a core layer of triphenyl phosphate (TPP), which blocks heat transfer[51]. The shell layer is a mixture of PVDF, SiO_2, and graphene oxide (GO), ensuring efficient migration of Li^+ while maintaining high-temperature stability, and its exposure to the outside can speed up the flame-retardant response.

ELECTROSPUN FIBER AS CATHODE MATERIALS

Electrospinning technology is an important synthetic method for preparing fiber-based cathode materials, and it is often used in the production of FLBs[18,52]. This technology uses an electric field to deposit the precursor solution through the nozzle onto the substrate, forming the deposition and connection of nanofibers. Since the precursor solution can be combined with the precursor of the cathode, the size, shape, and bonding between the cathode material and the fiber can be improved by adjusting the proportion of the precursor solution, the electrospinning voltage, and the receiving substrate. Therefore, electrospinning technology is considered to have great potential in the field of flexible cathodes and has received widespread attention. This section will review its application in fiber-based cathodes.

Pre-spinning solution loaded with cathode materials

In the application of electrospinning technology, a pre-spinning solution loaded with active cathode material is the simplest and most direct method of cathode synthesis. The nanoscale cathode active particles that can pass through the nozzle of the electrospinning machine can be directly added to the pre-spinning solution, and the fibers with active cathode materials can be obtained by adjusting the spinning parameters.

Li_2MnSiO_4 (LMS) has a high theoretical specific capacity (332 mAh g^{-1}), and its conductivity can be improved through iron doping[53]. $Li_2Mn_{0.8}Fe_{0.2}SiO_4$/polyacrylonitrile (PAN) composite nanofibers were prepared by mixing $Li_2Mn_{0.8}Fe_{0.2}SiO_4$ with PAN solution as active cathode material. Then, $Li_2Mn_{0.8}Fe_{0.2}SiO_4$/carbon composite nanofibers were obtained by carbonization at 700 °C for 8 h in argon atmosphere. The $Li_2Mn_{0.8}Fe_{0.2}SiO_4$ nanoparticles were embedded in carbon nanofibers (CNFs) to achieve a binder-free cathode, demonstrating a high specific capacity of 224 mAh g^{-1}. LMS can also be synthesized with solvothermal methods, which can be combined with PAN to obtain the final LMS/CNFs by electrospinning and high-temperature carbonization[54]. The application of electrospinning technology not only realizes one-dimensional directional arrangement of LMS nanorods, but also produces conductive CNFs through carbonization, providing an excellent electron transport channel for LMS nanorods.

In the above work, a high-temperature post-treatment step is conducted after electrospinning, which can achieve uniform dispersion of the cathode particle in carbon-based materials, improve conductivity, and

alleviate the pulverization of cathode particles caused by volume changes. However, the removal or carbonization of polymers that can act as binders may lead to brittleness of fibers and fiber networks, so additional binders may be needed to prepare the cathode of FLBs. The retention of polymer structures in nanofibers may be one of the solutions to achieve cathode flexibility and strong anchoring of active materials in fibers.

Mados *et al.* prepared a pre-spinning solution by mixing $LiFePO_4$ (LFP) powder with Super C65 and multi-walled carbon nanotubes (MWCNTs) conductive agent and PEO binder in a mixture of chloroform and N,N-dimethylformamide (DMF)[55]. The self-supporting fiber network cathode [LFP/current collector (CC)] is directly obtained by two types of electrospinning methods (bilayer and interlayer) without post-treatment [Figure 4A]. Focused ion beam-scanning electron microscope-energy dispersive spectrometer (FIB-SEM-EDS) images [Figure 4B] exhibited well-dispersed LFP particles and highly porous structure on the fibers, which promoted electrolyte penetration, thus achieving full utilization of the active sites inside the fibers. 35 × 55 mm^2 nonwoven mesh of LFP cathode does not produce fiber tearing after folding and twisting [Figure 4C]. In addition, by comparing the arrangement of different collectors and cathodes, the authors find that compared with the bilayer structure, interlayered LFP/CC structure has more contact area to build a better 3D conductive network, showing excellent electrochemical performance.

The pre-spinning solution can be prepared by mixing nano graphite particles and carbon-coated LFP/C nanoparticles with PVDF-HFP precursor solution[56]. Through electrospinning technology, the pre-spinning solution of the anode, separator and cathode is deposited on the copper mesh CC in turn, and then immersed in the liquid electrolyte to achieve the preparation of "all-in-one" FLBs [Figure 4D]. The authors optimized the length and diameter of the nanofibers and controlled component thickness [Figure 4E] by optimizing electrospinning parameters such as voltage, needle-to-collector distance, and solution flow rate. The electronic conductivity of the fiber electrode was increased by adding carbon nanotubes (CNT) into the electrospinning solution. The transmission electron microscope (TEM) images in Figure 4E exhibit that the particles of the active material are tightly coated by the polymer, and this strong anchoring helps ensure that the active material will not detach during bending. After 40 times bending tests, the potential of the FLBs remained stable, showing good mechanical flexibility and electrochemical stability.

Most studies on pre-spinning solutions loaded with inorganic cathode nanoparticles need to address issues such as mixing with spinning solution, contact with the conductive agent and the spatial relationship between cathode nanoparticles and fibers. Because the polymer cathode content does not affect the continuity of the electrospinning fiber, the energy density reduction caused by the use of inactive components can be significantly mitigated. Therefore, polymer-based flexible cathodes are attracting considerable attention.

For example, polyindole, a conductive electroactive polymer, can be used as the active cathode material, and can be synthesized into nanofibers anode by electrospinning technology[57]. The authors achieved smooth fibers by regulating the concentration of polyindole solution, and found that the electronic conductivity of the electrode was affected by the geometric structure of the fiber and electrode. The polymer electrode achieves a specific capacity of 79 mAh g^{-1} at 200 mAg^{-1}, which is 94% of the theoretical capacity.

Flexible polymer cathodes with polytriphenylamine (PTPA) and its derivative [PTPA-3-carboxyl-2,2,5,5-tetramethyl-3-pyrrolin-1-oxyl (PO)] as active materials, and CNTs as conductive fillers can be fabricated by nonsolvent induced phase separation electrospinning (NIPSE) method[58]. The polymer cathode fibers achieved through direct electrospinning exhibit a porous structure. Furthermore, the authors found that by

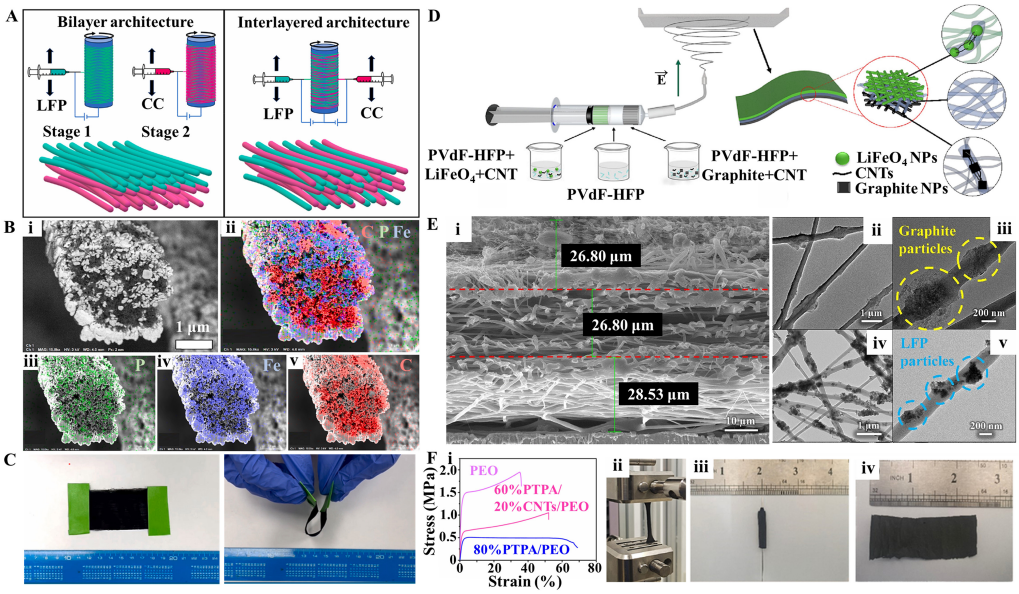

Figure 4. (A) The self-supporting fiber network cathode (LFP/CC) obtained by two types of electrospinning methods (bilayer and interlayer). (B) The FIB-SEM-EDS images of LFP/CC. (C) The folding and twisting tests for 35 × 55 mm^2 nonwoven mesh of LFP/CC cathode[55]. Copyright 2024, Elsevier. (D) The fabrication method of "all-in-one" FLBs. (E) The TEM images of fiber cathode and fiber anode in "all-in-one" FLBs[56]. Copyright 2023, Elsevier. (F) Stress-strain test and winding test of PTPA-PO cathode[58]. Copyright 2024, Elsevier.

adjusting the content of CNTs and PEO, a composite film containing 20% CNTs exhibits a high tensile strength of 1.05 MPa and can adapt to stretching and winding without damage, demonstrating good flexibility [Figure 4F], which enable the polymer cathode to achieve a discharge capacity of 114.6 mAh g^{-1}, a capacity retention of 93.3% after 100 cycles, and a low charge transfer resistance (Rct, 120 Ω).

Electrospinning-assisted cathode preparation

Directly mixing the cathode active materials with the pre-spinning solution and then using electrospinning technology to achieve fiber cathodes is a simple method. However, due to the difficulty in controlling the compatibility between particles and the pre-spinning solution and ensuring the reliability of the bonding between cathode particles and fibers after spinning, the direct electrospinning method with cathode particles is challenging to meet the large-scale preparation of flexible cathodes. Some cathodes with specific sizes or special physicochemical properties may not be suitable for direct spinning. In addition to directly carrying cathode particles, electrospinning technology can also assist in the synthesis of flexible cathodes. For example, spinning the precursors of cathode materials and then conducting post-treatment to achieve flexible cathodes further expands the possibilities of electrospun cathodes.

Polyanionic compounds such as LMS, LFP, $Li_3V_2(PO_4)_3$ (LVP), *etc.*, have attracted the attention of researchers due to their good thermal stability, high electrochemical stability, and wide voltage plateau. For instance, LMS is of particular interest to researchers in flexible energy storage because of its high theoretical capacity (333 mAh g^{-1}) and excellent thermal stability. However, the Jahn-Teller distortion caused by Mn^{3+} in its structure and its low electrical conductivity limit its practical application. Park *et al.* prepared LMS/C nanofibers by mixing lithium acetate and manganese acetate precursors into the electrospinning solution, followed by electrospinning and subsequent carbonization processes, which effectively improved the electrochemical performance of LMS, achieving 314 mAh g^{-1} at 0.05 C (16.5 mA g^{-1}) in the initial cycle[59].

Olivine-structured LFP, as a representative of phosphate-based cathode materials, is a commonly commercialized low-cost and high-safety cathode with a broad research foundation and a complete industry chain. Therefore, using it as a flexible cathode active material is highly feasible and adaptable. The precursors [Li($COOCH_3$), Fe($COOCH_3$)$_2$, and H_3PO_4] with pre-spinning solution can be combined to prepare LFP-CNF composites through electrospinning and subsequent heat treatment[60]. By adjusting heat treatment parameters such as heating rate, carbonization temperature, and holding time, the authors were able to control the crystal structure, morphology, and electrochemical performance of the composites. The LFP-CNF composites carbonized for 14 h at 800 °C in argon demonstrated flexibility and the highest discharge capacity. In addition, LFP@reduced GO (rGO)/CNFs flexible cathodes can be prepared by combining $FeC_6H_5O_7$ and LiH_2PO_4 precursors with pre-spinning solution, followed by electrospinning and high-temperature pyrolysis[61]. LFP nanoparticles are tightly attached to CNFs with the help of electrostatic interactions, and CNFs are fused to form interconnected carbon layers attached to the rGO surface. The tailored structure achieved enhanced electronic conductivity and unobstructed Li^+ transport pathways, realizing a high-rate flexible cathode that still provides a high capacity of 118.9 mAh g^{-1} at 10 C. Kwon *et al.* fabricated SnO_2/C nanofiber anodes and LFP/C nanofiber cathodes through electrospinning and high-temperature treatment, and integrated them with a stretchable gel polymer electrolyte to achieve a stretchable Li-ion full cell[62]. The combination of LFP with a carbon layer achieved an effective conductive carbon network, and the resulting FLBs exhibited high mechanical strength and voltage stability [Figure 5A and B], demonstrating a high capacity of 128.3 mAh g^{-1} even under a 30% stretch while continuously powering a light emitting diode (LED) [Figure 5C].

However, Hongtong *et al.* believed that composite fibers composed of LFP and carbon might not be sufficient to overcome the main drawback of the low electronic conductivity of olivine compounds[63]. Therefore, the authors constructed a unique core-shell LFP/FeS/C composite material through electrospinning and high-temperature pyrolysis, and they detailed the impact of Na^+, Mg^{2+}, and Al^{3+} ions on the structure, morphology, and electrochemical properties. The authors found that the uniform distribution of FeS in the core of the composite fibers enhanced the electronic conductivity of the fibers, and they discovered that the doping of high-valence Al^{3+} could induce lattice expansion and the formation of lithium vacancies, thereby achieving higher ionic conductivity. The cathode with 5% Al^{3+} doping provided a specific capacity of 155 mAh g^{-1} at 0.2 C, which is close to the theoretical capacity of LFP, 170 mAh g^{-1}. Similarly, Mn-doped LFP can be synthesized through electrospinning of precursors and subsequent heat treatment at 600 °C[64]. The occupation of the Fe site in LFP by Mn^{2+} induces lattice distortion, leading to the formation of a Li(FeMn)PO_4 (LFMP) solid solution. The expansion of the lattice facilitates the insertion/deinsertion of Li, thereby improving the ionic conductivity of LFP and reducing polarization during the Li insertion/extraction process. This results in a capacity of 160.3 mAh g^{-1} being maintained after 200 cycles at 0.1 C.

LVP, as another common phosphate-based cathode material, possesses a relatively high reaction potential (≈3.8 V *vs.* Li^+/Li) and a larger theoretical capacity (197 mAh g^{-1}). However, it also suffers from the inherent low electronic conductivity characteristic of phosphate cathodes. Therefore, Shin *et al.* successfully controlled the microstructure of the LVP-CNF composite by adjusting the sintering parameters, enabling the growth of LVP on CNFs with some particles protruding from the fibers, which is beneficial for the rapid diffusion of Li^+ and efficient electron transport[65]. Lokeswararao *et al.* further improved the rate performance (58.74 mAh g^{-1} at 10 C) of LVP by controlling the connectivity and microstructure of LVP with carbon fibers, maintaining a capacity retention of 77.2% after 500 cycles at 1 C[66]. In addition to carbon coating modification, Gavali *et al.* demonstrated through calculations that doping with boron can reduce the diffusion barrier of LVP and increase the specific capacity to 205 mAh g^{-1}[67].

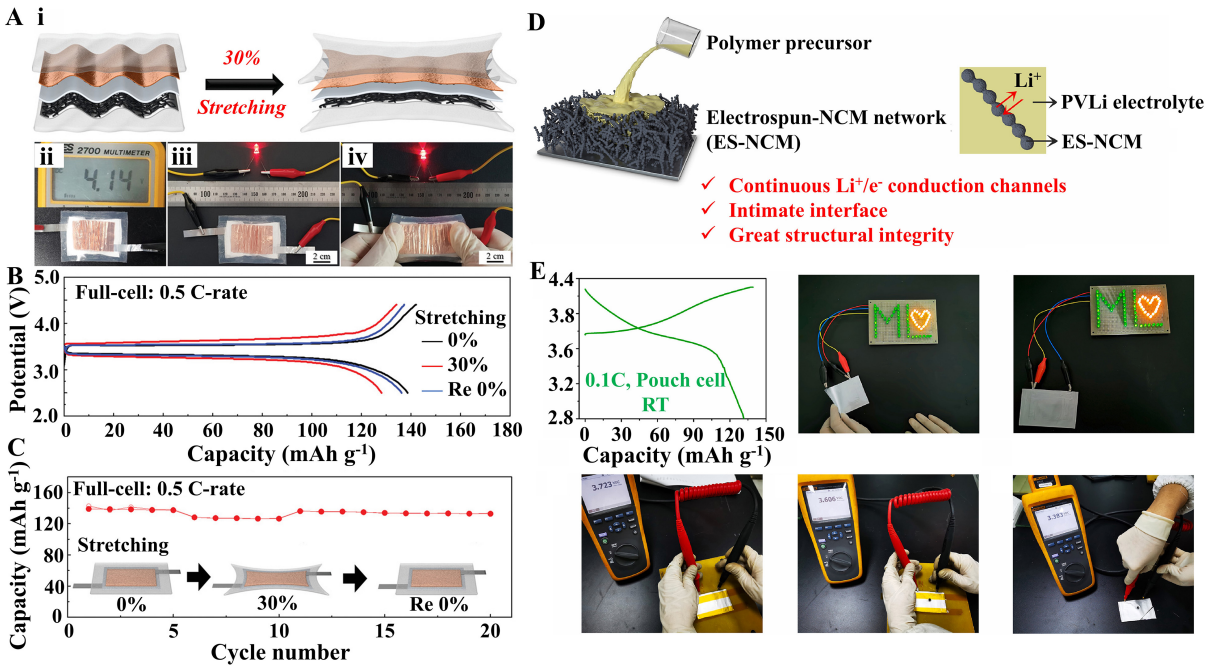

Figure 5. (A) The schematic diagram and tensile tests of the stretchable Li-ion full cell assembled with SnO_2/C nanofiber anode, LFP/C nanofiber cathode and a stretchable gel polymer electrolyte. (B) The potential curves of the stretchable Li-ion full cell with various stretching ratios. (C) The cycle stability of the stretchable Li-ion full cell with various stretching ratios[62]. Copyright 2020, Wiley. (D) The *in-situ* polymerization of polymer precursor solution in the cross-linked skeleton composed of NCM nanoparticles. (E) The charge-discharge curves of the flexible Li-ion pouch cell and nail penetration and cutting tests of flexible Li-ion pouch cell[75]. Copyright 2022 Elsevier.

In addition to phosphate cathodes, transition metal oxide cathodes such as LCO and $LiNi_xCo_yMn_{1-x-y}O_2$ (NCM) are commonly used commercial cathode materials, often utilized for energy storage in electric vehicles and 3C devices. The spinel-phase cathode material $LiMn_2O_4$ belongs to the cubic crystal system, with an Fd-3m space group[68]. In the highly delithiated state, the presence of Mn atoms in every layer of the structure provides excellent support, effectively maintaining structural stability. However, the lattice distortion caused by the Jahn-Teller effect means that commercially available $LiMn_2O_4$ can only be used within a voltage range above 3 V. Porous hollow nanofibers can be synthesized through electrospinning of precursors and subsequent heat treatment, effectively alleviating structural strain and volume changes, achieving long-term cycling stability, and demonstrating a capacity of 105.2 mAh g^{-1} after 400 cycles at 0.1 C[69]. In order to achieve spinel-phase cathode materials with more stable structures and higher energy densities, researchers have replaced Mn with Ni elements to obtain $LiNi_xMn_{2-x}O_4$ (LNMO), which also has a spinel structure. This substitution promotes the oxidation of Mn, thereby significantly suppressing the Jahn-Teller effect of Mn^{3+}. Xu *et al.* have developed the great potential of electrospinning, synthesizing LNMO nanofibers with diameters as thin as 50 nm by adjusting and controlling the heating process[70]. To address the low electronic conductivity and volume change issues of LNMO at 3 V or lower voltages due to phase transitions, the composition of interconnected polycrystalline LNMO nanoparticles with CNTs can be synthesized through electrospinning of precursors and subsequent heat treatment, forming 1D LNMO nanofibers that exhibit a capacity of 134 mAh g^{-1} at 0.1 C[71].

Layered oxides, represented by $LiMO_2$ (M = Co, Ni, or Mn), are a typical type of cathode material for LIBs. Among them, LCO, as one of the most successful commercial layered cathode materials, was first reported by Mizushima *et al.* in 1980 and was first commercialized by Sony Corporation of Japan in 1991, paired with

a graphite anode[72]. LCO nanofibers can be synthesized through electrospinning and heat treatment at 700 °C, achieving high specific capacity by adjusting the Li:Co ratio and sintering temperature[73]. Min *et al.* found that the formation of effective conductive nanofibers during the electrospinning synthesis of $Li_{1.2}Ni_{0.17}Co_{0.17}Mn_{0.5}O_2$ nanowires is beneficial to intercalation kinetics[74]. In addition, a cross-linked skeleton composed of NCM nanoparticles can be prepared using electrospinning technology [Figure 5D], coordinating the decomposition of metal salts, polymer carbonization, and NCM crystal growth temperatures[75]. The porous morphology of NCM allows the polymer precursor solution to easily penetrate and *in-situ* polymerize, ensuring a continuous ion conduction channel. The solidified integrated composite cathode can be used to assemble FLBs. The flexible Li-ion pouch cell can deliver a specific capacity of 131.6 mAh g^{-1} at 0.1 C, maintain the lighting of a light-emitting diode (LED) when folded, and only experience a slight drop of open-circuit voltage without internal short-circuit after nail penetration and cutting [Figure 5E].

In addition, certain polymer cathodes can achieve reversible Li^+ storage through electron transfer redox reactions. For example, a fiber membrane obtained by loading polyimide (PI) on an electrospun CNF network exhibits a capacity of 170 mAh g^{-1} at 1 C, and retains 70.5% of its capacity at 100 C compared to that at 0.5 C[76]. The *in-situ* polymerization of polymers on flexible conductive substrates is a promising approach for the preparation of polymer-based flexible cathodes, offering broad research potential.

Self-supporting cathodes by electrospinning

Self-supporting cathodes, a special type of flexible cathode, do not rely on traditional metal CCs, reducing the mass of inactive components and thereby increasing the energy density of batteries[77]. Electrospinning is an effective method for preparing self-supporting cathodes, offering continuous production capabilities that enable large-scale preparation. Additionally, self-supporting cathodes produced through electrospinning often possess good flexibility, allowing FLBs to endure bending, folding, and twisting without compromising electrochemical performance. This feature is crucial for wearable and flexible electronic devices.

The aforementioned LFP can also be prepared as a self-supporting cathode using electrospinning technology. A flexible cathode with a self-supporting LFP/C nanofiber network can be fabricated through electrospinning, achieving LFP with a good Li^+ transport channel along the (010) plane through crystal engineering[78]. The self-supporting structure not only provides a fast Li^+ diffusion path but also promotes the penetration of the electrolyte, maintaining a capacity retention of 98.2% after 500 cycles at 0.5 C. It is worth noting that hot pressing technology is often used in self-supporting fiber-based electrode materials because it can maintain the original shape of the fiber membrane and facilitate the cross-linking of polymers during heating, greatly suppressing the phenomenon of powder formation after calcination. The self-supporting LFP flexible cathodes and $Li_4Ti_5O_{12}$ (LTO) flexible anodes can be prepared through electrospinning and hot pressing, and fiber-based full cells made from the two electrodes showed stable electrochemical performance, demonstrating 100 mAh g^{-1} after 800 cycles at 1 C, indicating its application potential in the field of flexible batteries[79].

Additionally, LVP, known for its high energy density and long cycle life, can also be prepared into self-supporting structures with one-dimensional continuous electron transport pathways through electrospinning technology. Peng *et al.* successfully prepared self-supporting cathodes with LVP nanocubes embedded in N-doped CNFs (LVP-NC/NCNF) by introducing ILs during the electrospinning process[80]. ILs, as carbon sources, not only induce the formation of LVP nanocubes with (100) faces, but also can form N-doped biphasic carbon coatings during heat treatment, further enhancing the electronic conductivity of

the entire electrode, demonstrating a high discharge capacity of 143.6 mAh g^{-1} after 1,000 cycles at a rate of 5 C[80]. In addition, Ni nanoparticles were utilized as catalysts to prepare an LVP/C nanowire and nanofiber hybrid membrane with a 3D long-range conductive network and a mace-like fiber structure through an improved electrospinning method followed by hot-press sintering[81]. The good flexibility of this structure makes it suitable for FLBs. Table 1 summarizes the experimental method and electrochemical performance of cathode materials prepared by electrospinning. In summary, electrospinning technology has shown significant advantages in the preparation of self-supporting cathodes, including enhanced electron transport, increased contact area between the electrode and electrolyte, reduced electrode weight, and improved Li^+ transport pathways. Thus, it has attracted considerable attention from researchers and holds promising prospects.

ELECTROSPUN FIBER AS ANODE MATERIAL

Anode materials for FLBs can be categorized into intercalation-type, alloy-type, conversion-type, and other anodes, each with distinct lithium storage mechanisms. Many of these anodes, with varying lithium storage mechanisms, can be synthesized through electrospinning. Electrospinning, with its unique advantages, is widely used for preparing anodes for FLBs. This technique produces fiber-based anode materials with nanometer-scale diameters, high specific surface areas, and high porosity. Electrospinning shows great potential and advantages in the fabrication of anode materials for FLBs, with the electrochemical performance further optimized through material combinations and structural designs. The following will introduce the application of anodes with different lithium storage mechanisms for FLBs prepared via electrospinning.

Electrospun flexible anodes dominated by intercalation-type lithium storage

In the exploration of long cycle life anodes for FLBs, intercalation-type anodes, which store Li^+ through the intercalation mechanism, have demonstrated superior cycling retention and thus have attracted widespread attention from researchers. Intercalation-type anodes refer to the situation where Li^+ can be efficiently and reversibly stored in the vacant sites of the anode's host structure. For heterogeneous intercalation, the potential of the anode material remains essentially constant during the intercalation process, while for homogeneous intercalation, the voltage varies with the Li^+ content. These anodes, due to their specific framework, maintain good structural integrity during the insertion and extraction of Li^+, resulting in relatively small volume changes with voltages.

Moreover, for 1D intercalation-type anodes prepared by electrospinning, Li^+ and electrons can travel through the 1D fibrous pathways, which enhances rate performance. Although the capacity of intercalation-type anodes is limited due to the finite accommodation sites, they remain an attractive and competitive choice for portable flexible electronic devices that require safety, long cycle life, and rapid charging and discharging capabilities. Electrospun intercalation-dominated anode materials mainly include carbon-based materials, titanium-based materials, MXene, and others[82].

Carbon materials, as the most widely used anode materials to date, possess significant advantages such as low cost, widespread availability, good electrical conductivity, and strong structural stability, making them widely noticed as intercalation-type anodes in the field of FLBs. Biomass materials, such as cellulose and chitosan[83], which are abundantly available and can be added to the pre-spinning solution, are precursors for carbon materials. These can then be synthesized into clean, sustainable flexible CNF membrane anodes derived from biomass through high-temperature carbonization. In addition, low-cost carbon sources such as lignite and coal derivatives (e.g., humic acid and coal tar pitch) can also be used to prepare flexible self-supported carbon fiber anode materials[84]. The introduction of coal tar pitch into the electrospinning

Table 1. Experimental method, flexibility evaluation and electrochemical properties in LIBs of various cathode materials prepared by electrospinning

Materials	Experimental method	Flexibility evaluation	Capacity/current density/cycles	Ref.
$Li_2Mn_{0.8}Fe_{0.2}SiO_4$/carbon nanofibers	Electrospinning	-	171 mAh g^{-1}/16.65 mA g^{-1}/20	[53]
Li_2MnSiO_4 nanorods-embedded carbon nanofibers	Electrospinning	-	134 mAh g^{-1}/33.3 mA g^{-1}/150	[54]
Polymer-based $LiFePO_4$ cathode	Electrospinning	Foldable, twistable	118 mAh g^{-1}/10 μA cm^{-2}/1	[55]
$LiFePO_4$/C nanoparticles	Electrospinning	Foldable	140 mAh g^{-1}/1 C/200	[56]
Polytriphenylamine/carbon nanotube/polyethylene oxide	Electrospinning	Foldable, stretchable	109.7 mAh g^{-1}/20 mA g^{-1}/100	[58]
$LiFePO_4$-carbon nanofiber	Electrospinning + annealing	Flexible	146.3 mAh g^{-1}/0.5 C/100	[60]
$LiFePO_4$@rGO/carbon nanofibers	Electrospinning + annealing	Flexible	150 mAh g^{-1}/1 C/200	[61]
$Li_3V_2(PO_4)_3$/carbon nanofibrous	Sol-gel+ electrospinning + annealing	-	72.72 mAh g^{-1}/1 C/500	[66]
$LiMn_2O_4$ hollow nanofibers	Electrospinning + annealing	Flexible	105.2 mAh g^{-1}/0.1 C/400	[69]
$LiNi_{0.5}Mn_{1.5}O_4$ nanofiber/carbon nanotube	Electrospinning + annealing	-	66.44 mAh g^{-1}/14 mA g^{-1}/100	[71]
$Li_2CoTi_3O_8/TiO_2$ nanoparticles	Electrospinning + annealing	Flexible	68 mAh g^{-1}/0.1 C/25	[73]
$Li_{1.2}Ni_{0.17}Co_{0.17}Mn_{0.5}O_2$ nanofiber	Electrospinning + annealing	-	256 mAh g^{-1}/14.3 mA g^{-1}/1	[74]
$LiNi_{0.5}Co_{0.2}Mn_{0.3}O_2$ network	Electrospinning + annealing	Foldable	106 mAh g^{-1}/0.1 C/80	[75]
Polyimide/carbon nanofibers	Electrospinning + annealing	Flexible	170 mAh g^{-1}/1 C/1,000	[76]

solution enhances the flexibility and tensile strength of the carbon fibers, making them more suitable for FLBs. Moreover, coal tar pitch-derived carbon fibers (CTP-CFs) have a higher micropore surface area, higher pyridinic nitrogen content, and an optimal ratio of amorphous carbon (sp^3 carbon) to graphitic microcrystalline carbon (sp^2 carbon), demonstrating a high initial reversible capacity of 770.8 mAh g^{-1} at 20 mA g^{-1}. The use of low-cost precursors as carbon sources reflects the sustainability and environmental friendliness of carbon anodes. Additionally, it is worth noting that the control of electrospinning equipment parameters and the ratio of the electrospinning solution can achieve precise control over the structure of carbon materials. For instance, when preparing CNF membrane anodes using two different electrospinning nozzles (single and coaxial nozzles)[83], the single nozzle electrospinning method can more effectively dope bio-N into the CNF membrane anode. By adjusting the mass ratio of cellulose and chitosan, high specific capacities of 401 and 210 mAh g^{-1} at 30 and 1,000 mA g^{-1} can be achieved respectively. Furthermore, the electrospinning parameters such as liquid flow velocity, voltage, and drum speed can be adjusted to control the nanostructure of PAN-derived flexible CNFs [electrospun PAN (ES-PAN)][85]. Their disordered porous nanostructure and large specific surface area enable the ES-PAN electrode to exhibit an initial charge capacity of 404.7 mAh g^{-1} at 0.2 C. In contrast to the common synthesis methods using PAN directly, the flexible CNFs formed by carbonizing the PI derived from the ES-PAN fiber film after imidization at 350 °C for 1 h show a reversible capacity of 710 mAh g^{-1} at 0.05 A g^{-1}, holding promise for achieving high-energy-density FLBs[86].

Besides carbon materials, titanium-based flexible anode materials are also important intercalation-type anodes. Electrospinning can be used to prepare flexible anodes based on nanotubular structures of TiO_2 with self-supporting characteristics[87]. By optimizing the electrospinning parameters, complete nanofiber anodes that are not agglomerated and are fully coated with TiO_2 nanotubes can be obtained. The preparation of TiO_2 flexible anodes without additional CCs and binders reduces the weight of cells and has potential application value in flexible electronic devices. To further improve the electronic conductivity and enhance the high-rate performance of titanium-based anodes, the design of heterostructures is an approach.

Heterogeneous structures of LTO/rutile TiO_2 (LTO/RT) can be prepared by electrospinning technology[88]. The construction of the heterostructure interface significantly improves electronic conductivity and Li^+ diffusion, achieving a capacity of 125.5 mAh g^{-1} after 500 cycles at 10 C. In the aforementioned research, although the zero-strain characteristics of TiO_2 contribute to a high cycling retention rate, its capacity does not meet the demands of FLBs. Therefore, other titanium-based flexible materials, such as the perovskite-type $Na_{0.35}La_{0.55}TiO_3$, have been designed and studied[89]. Similar to TiO_2, the $Na_{0.35}La_{0.55}TiO_3$ material embedded in multi-channel carbon fibers synthesized by the electrospinning method also has zero-strain characteristics and exhibits a higher capacity (265 mAh g^{-1} at 0.1 A g^{-1}). In addition, its highly reversible solid-solution reaction mechanism and stable Ti-O framework [Figure 6A] ensure that this flexible anode has a high cycling retention rate (96.3% after 9,000 cycles at 2 A g^{-1}). The full cell, composed of this material and LFP, exhibits excellent rate performance [Figure 6B and C], delivering a reversible capacity of 116 mAh g^{-1} at 1 A g^{-1}.

MXene, as an emerging two-dimensional material, has been considered a promising candidate for flexible anode materials in LIBs due to its excellent electrical conductivity, large specific surface area, and abundant surface functional groups. Typically, MXene is prepared by selectively etching the "A" layer (such as Al) in the MAX phase, resulting in a material with high electrical conductivity and lithiophilic properties. However, the interlayer van der Waals forces of MXene nanosheets can lead to restacking in practical applications, causing structural collapse and affecting capacity performance[90]. To address this issue, researchers have employed various strategies. For instance, the fabrication of flexible 3D anodes through electrospinning technology, which interweaves conductive hollow copper/CNTs with MXene [Figure 6D][91], not only provides a cross-network for rapid electron diffusion but also restricts the stacking of MXene through unique structural design, thereby alleviating volume expansion during cycling. Moreover, carbon-coated MXene synthesized via electrospinning exhibits a 3D network structure interwoven with nanofibers[92], significantly resolving the poor penetration and diffusion of the electrolyte caused by the stacking issue of MXene. This has enabled the realization of high-performance flexible self-supported anodes with capacities exceeding 600 and 400 mAh g^{-1} at 0.1 and 2 A g^{-1}, respectively.

Electrospun flexible anodes dominated by alloy-type lithium storage

The alloy-type lithium storage mechanism refers to the metal/non-metal anode, which can form an alloy with Li during the cycling process, thereby storing Li in the form of an alloy. Due to the solid solution reaction typically being able to store a sufficient amount of Li, alloy-type anodes usually have a very high reversible specific capacity, thus gaining attention in high-energy-density FLBs. The alloy-type anodes mainly include tin (Sn)-based, silicon (Si)-based, germanium (Ge)-based, and other anodes. However, during lithium storage of alloy-type anodes, the influx of atoms into the alloy often causes a significant volume change, sometimes reaching as much as 300%-400%. Without a reasonable structural design, alloy-type anodes can lose electrical contact due to the detachment of powder, leading to a rapid decline in the capacity of FLBs. Therefore, researchers focus on the structural optimization of alloy-type anodes to achieve volume buffering.

Sn-based anodes, due to their high theoretical specific capacity (the theoretical capacity of Sn is 994 mAh g^{-1}), low electrochemical potential, and abundant crustal reserves, have become an attractive anode material for FLBs. However, these anodes face the common problem of alloy-type anodes; that is, during the charge and discharge, the volume change of Sn-based alloys can reach 200%-300%. This leads to the fragmentation and pulverization of the electrode material, thereby increasing the internal resistance of the battery and reducing cycle stability. In addition, it is worth noting that due to the formation of the solid electrolyte interphase (SEI) film in the initial cycle, the coulombic efficiency of Sn-based alloy anodes is usually low. To address these issues, researchers have designed the structure of Sn-based anodes based on

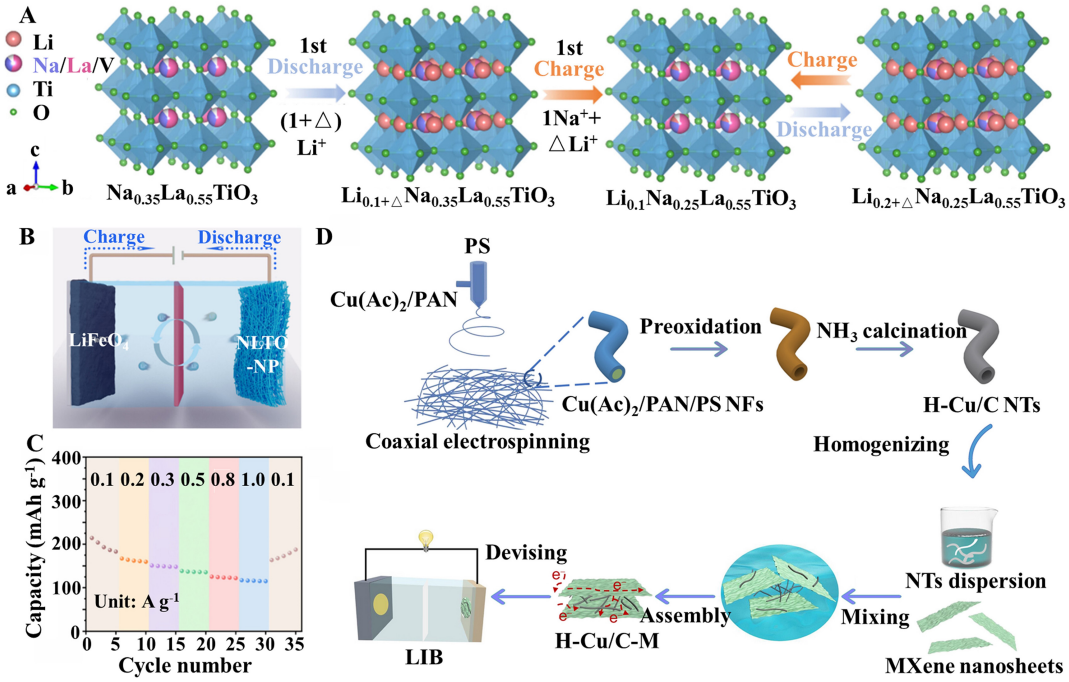

Figure 6. (A) The reversible solid-solution reaction mechanism of $Na_{0.35}La_{0.55}TiO_3$ material. (B) The schematic diagram of full-cell composed of $Na_{0.35}La_{0.55}TiO_3$ and LFP. (C) The rate performance of full-cell[89]. Copyright 2024 American Chemical Society. (D) The schematic diagram of the fabrication of flexible 3D hollow copper/carbon nanotubes with MXene anodes[91]. Copyright 2023, Springer Nature.

electrospinning technology, preparing nanofibers with good mechanical flexibility and controllable structure to solve the aforementioned problems.

In the field of anode material structural optimization, researchers have paid special attention to carbon materials, which are used to alleviate the volume expansion problem of Sn-based anodes due to their excellent structural stability and electrical conductivity. By combining electrospinning technology with heat treatment, Sn/C fiber films can be prepared[93], in which the use of folic acid and polymethyl methacrylate not only achieves nitrogen doping of Sn/C but also promotes the formation of a porous structure. The construction of this 3D carbon fiber conductive network plays a significant buffering role in alleviating stress changes caused by volume expansion and effectively prevents the aggregation of Sn nanoparticles. This anode material, after 500 cycles at 500 mA g^{-1}, still exhibits a discharge capacity of 712.1 mAh g^{-1}, significantly demonstrating its great application prospect as a high-performance self-supporting flexible anode material.

Similarly, composite materials of Sn-based metal-organic frameworks (Sn-MOFs) and CNFs prepared via electrospinning and carbon thermal reduction can yield self-supporting porous membranes[94]. Sn-MOFs not only serve as a Sn source but also, after pyrolysis, derive a porous carbon structure encapsulating Sn nanoparticles, greatly mitigating the severe volume changes during the cycling process. The self-supporting anode formed by electrospinning exhibits excellent mechanical toughness, with no significant resistance changes after 210 bending cycles [Figure 7A], and the pouch FLBs assembled with it show similar cycling performance to unbent batteries after multiple bending cycles [Figure 7B], demonstrating its potential in the field of flexible energy storage.

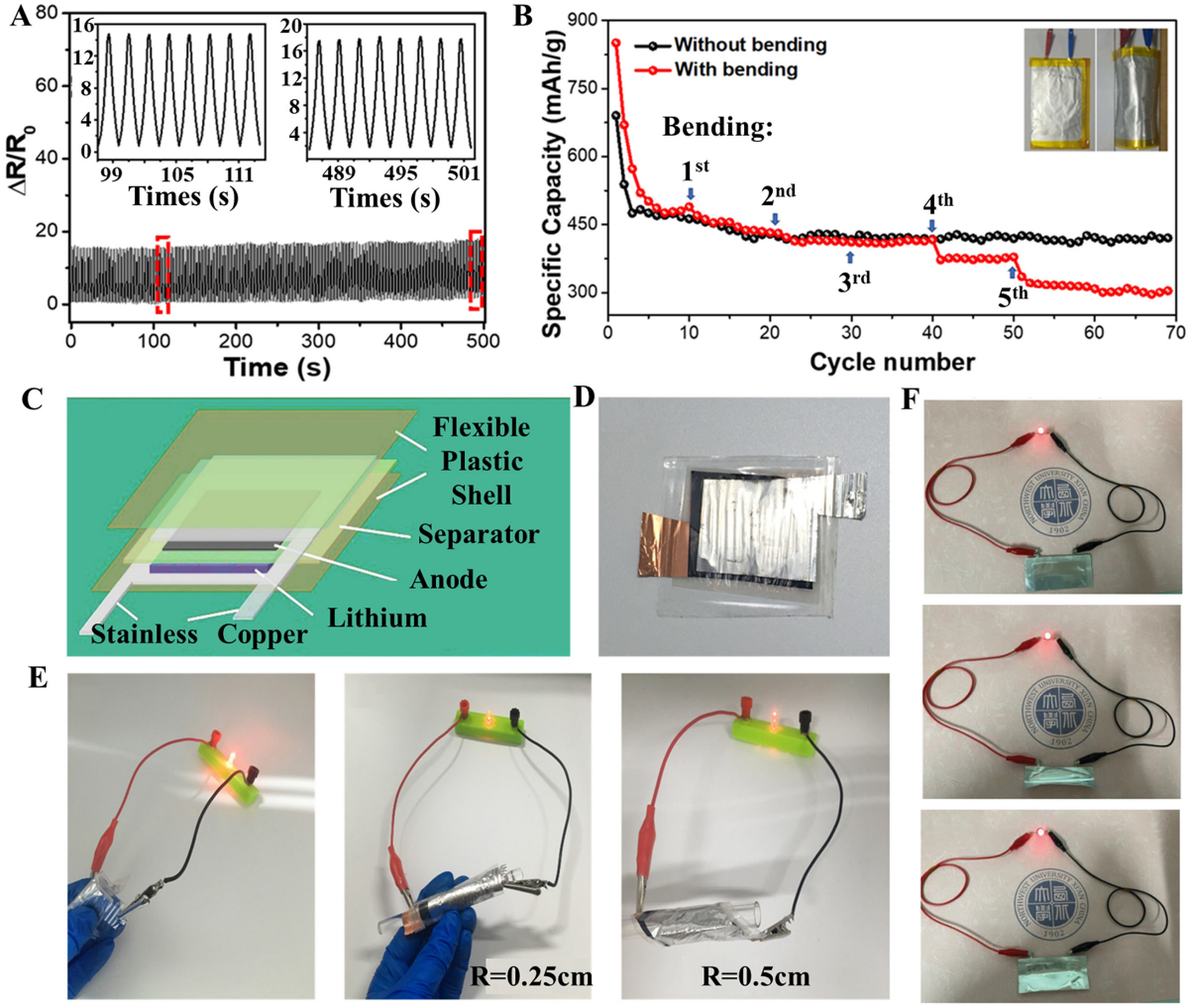

Figure 7. (A) The resistance test of self-supporting Sn-MOF anode. (B) The cycle test of pouch FLBs assembled with self-supporting Sn-MOF anode under multiple bending[94]. Copyright 2021 IOP Publishing. (C and D) The schematic diagram and digital photo of FLBs assembled with Si@C anode. (E) The LED lighting up tests of FLBs with Sn-MOF anode under bending conditions[97]. (F) The LED lighting up tests of FLBs with three-dimensional interconnected silicon/carbon network anode under bending conditions[101]. Copyright 2021 Wiley.

In addition to carbon material encapsulation, constructing intermetallic compounds is also an important means to alleviate the large volume changes of pure Sn-based anodes during the cycling process. The volume change of the Sn-Cu alloy is reduced by 140% compared to that of pure Sn anodes during the Li insertion and extraction. Composite nanofibers prepared by electrospinning technology, with Sn-Cu alloy particles uniformly encapsulated in CNFs[95], optimize the performance of Sn-based alloy anodes, demonstrating a discharge specific capacity of 501.8 mAh g^{-1} after 100 cycles at 100 mA g^{-1}.

Si-based anodes, due to their high abundance, high theoretical capacity (4,200 mAh g^{-1} for $Li_{4.4}Si$), and lithiation potential close to graphite, have been preliminarily attempted for large-scale application in the energy storage field of portable electronic devices. However, due to the excessive volume changes of Si and SiO_x during cycling, the actual amount of Si-based materials added to the anode is not high enough to ensure cycle life. In addition to the volume issue, the low electrical conductivity of Si also affects the performance, especially under high-rate conditions. Therefore, researchers have made many efforts to solve

the aforementioned problems[96]. Among them, the structural design of Si-based materials can improve structural stability. For example, Si@C core-shell structured nanofibers prepared by electrospinning technology can effectively alleviate the volume expansion of silicon nanoparticles during the charge and discharge, while enhancing structural stability and electron transfer rate[97]. The core-shell structured Si@C anode can still deliver 7,624 mAh g^{-1} after 100 cycles at 0.1 A g^{-1}. Moreover, FLBs assembled with Si@C [Figure 7C and D] exhibit stable cycling performance under bending conditions, with no significant capacity loss, and can light up commercial LEDs [Figure 7E]. In addition to the core-shell structure, the design of porous structures also helps to buffer volume changes, increase the contact area with the electrolyte, and improve the diffusion rate of Li^+[98]. Taking the Si@SiO_x/CNF flexible film prepared by electrospinning technology as an example[99], Si@SiO_x particles are generated during the oxidation phase and embedded in a matrix composed of CNFs, constructing a 3D reticular structure. The high porosity of this porous electrode material helps prevent the fragmentation of silicon particles.

Structural designs including core-shell structures and porous structures play an important role in solving volume change issues, and it is worth noting that the problem of poor conductivity also needs to be addressed urgently. The construction of conductive networks can be achieved through electrospinning technology[2]. For example, in the Si@SiO_2@CNF composite anode prepared by electrospinning, Si nanoparticles are uniformly dispersed in CNFs[100]. The interconnected conductive CNFs not only improve the conductivity of the anode, achieving a capacity of 903.7 mAh g^{-1} after 200 cycles at 100 mA g^{-1}, but also withstand multiple bendings without breaking. In addition, the 3D interconnected silicon/carbon network constructed by self-assembled microspheres and interwoven N-doped CNFs provides a fast ion/electron transfer channel[101]. The FLBs assembled with this network deliver 450 mAh g^{-1} after 200 cycles at 0.5 A g^{-1}, and can power an LED under bending conditions [Figure 7F], indicating excellent flexibility of the electrode.

Compared to the poor electrical conductivity of Si-based materials, Ge-based materials show great potential in FLBs due to their higher electronic conductivity, lower Li^+ diffusion barriers, and high theoretical capacity (1,624 mAh g^{-1}). During the charging and discharging of Ge-based materials, the pulverization of electrode materials caused by volume expansion can lead to a loss of electrical contact and capacity decay. Additionally, it can induce continuous side reactions at the fracture points, resulting in the formation of loose and relatively thick high-resistance SEI. Similar to the aforementioned Sn-based and Si-based anodes, researchers often use electrospinning technology to construct carbon-coated or 3D supporting structures. In the N, S co-doped Ge and porous CNF composite prepared by electrospinning technology, the porous CNFs provide good mechanical support to alleviate the volume expansion of Ge[102]. In addition, the carbon coating layer further prevents direct contact between Ge and the electrolyte, mitigating the continuous occurrence of adverse side reactions, and still provides a high reversible capacity of 795.9 mAh g^{-1} after 100 cycles at 100 mA g^{-1}.

Electrospun flexible anodes dominated by conversion-type lithium storage

In FLB anodes, conversion-type lithium storage is primarily dominated by transition metal compounds, such as oxides, sulfides, phosphides, *etc*. During the reaction with Li, the transition metal is reduced, and Li is oxidized to form a lithide. This conversion reaction enables conversion-type anodes to provide high capacity. While the conversion of Li causes volume expansion in the anode, it is less significant than the expansion observed in alloy-type anodes, resulting in a lower cycle decay than that of alloy-type anodes. The main contradiction of conversion-type anodes lies in the inevitable voltage hysteresis, which is mainly related to the electronegativity of anions and ion conductivity. Therefore, when designing flexible conversion-type anodes, researchers must address the issues of alleviating volume changes and voltage hysteresis.

Transition metal oxides are widely available, easily synthesized, and cost-effective conversion-type anode materials that offer high theoretical capacities. Common conversion-type oxide anodes mainly include iron-, cobalt-, and manganese-based oxides, among which iron-based oxides, such as Fe_3O_4 and Fe_2O_3, have attracted widespread attention from researchers due to their high theoretical specific capacities (915 and 1,007 mAh g^{-1}) and the abundance of iron resources. However, iron-based oxides undergo significant volume changes during the charge and discharge, which can lead to structural fragmentation and performance degradation. To address this issue, researchers have coated the iron-based oxides with carbon layers to improve their structural stability[103]. For example, in the 3D porous carbon-coated Fe_2O_3 anode prepared by electrospinning and carbonization, Fe_2O_3 is completely encapsulated within closely contacted CNFs [Figure 8A], and this 3D network structure not only prevents the aggregation of Fe_2O_3 nanoparticles but also provides an effective ion transport pathway[104]. Based on carbon composites, researchers have also improved the cycle stability by compounding iron-based oxides with other active materials, such as manganese-based oxides[105]. The Fe_3O_4/Fe_3C/MnO/CF composite anode prepared by the electrospinning method combines the high theoretical specific capacity of Fe_3O_4 and MnO, the good conductivity of Fe_3C, and the mixed mitigation of volume expansion of iron compounds by carbon coating and MnO, jointly enhancing the electrochemical performance of the flexible anode, achieving a high specific capacity of 750.23 mAh g^{-1} after 200 cycles at 0.2 A g^{-1}. It is worth noting that the poor conductivity of iron-based oxides themselves can be achieved by constructing a conductive network[106]. For example, in the flexible anode composed of rGO and Fe_3O_4 nanoparticles[107], the high conductivity of rGO is key to improving the conductivity of the composite material, and the good interfacial action between rGO and Fe_3O_4 also helps improve the efficiency of electron transfer. In addition to iron-based oxides, common oxide conversion-type anodes include Co_3O_4, MnO_x, *etc.*[108], which also face challenges such as volume expansion during charging and discharging, inherent poor electronic conductivity, and poor ionic conductivity. Researchers often design their nanostructures based on electrospinning and improve their reversible capacity and cycle stability by compounding them with carbon materials, MXene, and other materials. To mitigate the volume expansion of Co_3O_4 during cycling and enhance its conductivity, Kim *et al.* utilized an electrospinning technique to coat Co_3O_4 with carbon nanopockets by dispersing a pre-spinning solution of carbon source, cobalt source, and carbon quantum dots (CQDs) within nanofibers [Figure 8B][109]. The CQDs induced the formation of carbon nanopockets within the CNFs, which not only increased the flexibility of the anode [Figure 8Ci] but also improved the conductivity of the Co_3O_4 anode (13.5×10^{-2} S cm^{-1}) [Figure 8Cii]. After enduring a continuous deformation/recovery test of 1,000 cycles using a micro-fatigue machine [Figure 8Ciii], the anode remained intact and demonstrated excellent electrochemical performance with 500 reversible cycles at 2 A g^{-1}.

Transition metal sulfides are another type of anode material based on conversion reactions, and their higher conductivity compared to transition metal oxides makes them more attractive. Factors that induce capacity decay, such as volume expansion, voltage hysteresis, and the generation of polysulfide anions, have attracted the attention of researchers. Similar to transition metal oxides, issues of volume expansion and voltage hysteresis can be addressed using solutions such as carbon coating[110], compounding with highly conductive active materials[111], and constructing better Li^+/electron transfer interfaces and pathways. The generation and shuttling of polysulfide anions are often controlled by nano-encapsulation or using specific separators[112]. Similarly, transition metal phosphides also face the inherent shortcomings of conversion-type anodes. Nano-structuring and compounding with carbon materials can improve their structural stability and reduce electron transfer resistance[113]. Other conversion-type anodes such as $ZnSnO_3$ can also store lithium in the following way:[114]

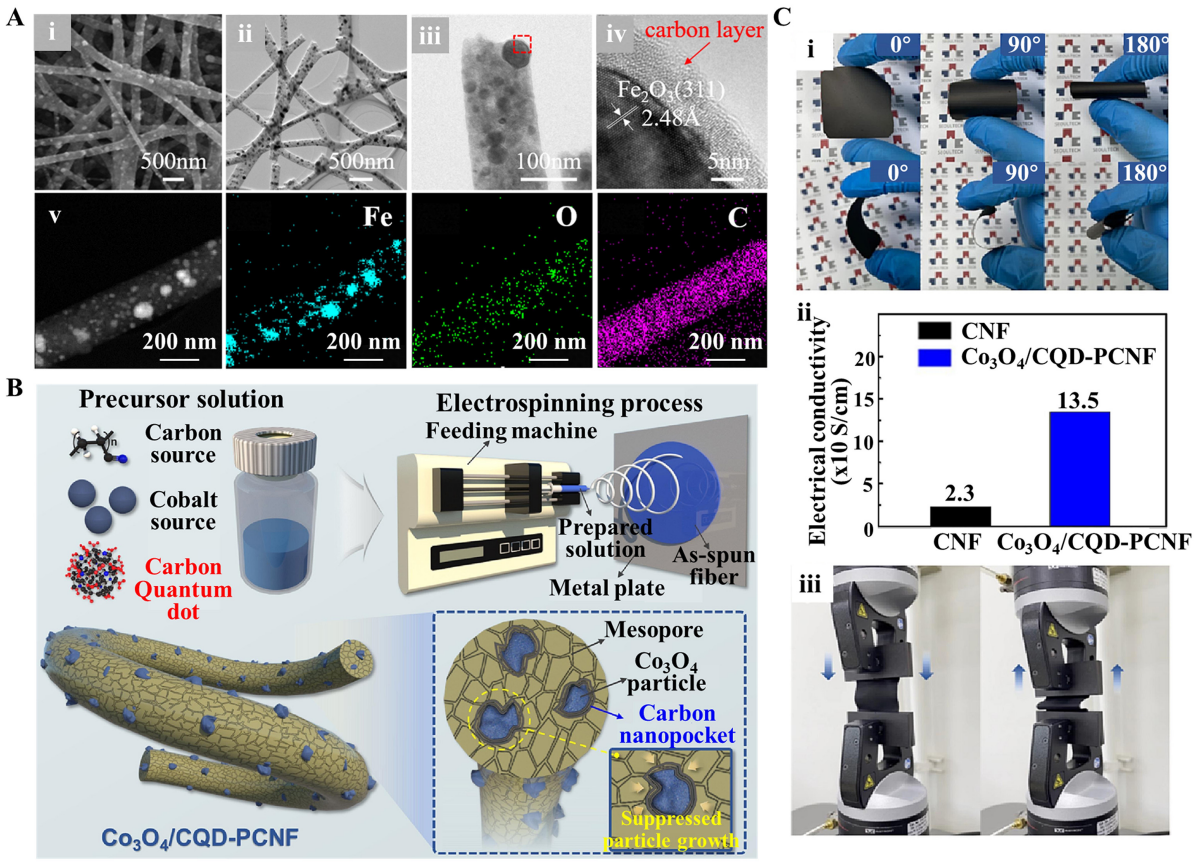

Figure 8. (A) The SEM and TEM-EDS images of a three-dimensional porous carbon-coated Fe_2O_3 anode[104]. Copyright 2020 IOP Publishing. (B) The schematic diagram of the manufacturing of Co_3O_4 coated with carbon nanopockets by electrospinning method. (C) The flexibility test, conductivity test, and deformation/recovery test of anodes[109]. Copyright 2023 Elsevier.

$$4Li^+ + 4e^- + ZnSnO_3 \leftrightarrow Sn + ZnO + 2Li_2O \quad (1)$$

$$6Li^+ + 6e^- + ZnSnO_3 \leftrightarrow Sn + Zn + 3Li_2O \quad (2)$$

$$xLi^+ + xe^- + Zn \leftrightarrow Li_{1-x}Zn,\ x \leq 1 \quad (3)$$

$$yLi^+ + ye^- + Sn \leftrightarrow Li_ySn,\ y \leq 4.4. \quad (4)$$

Encapsulating $ZnSnO_3$ micro-cubes in N-doped CNF membranes can effectively address volume expansion, enhancing structural stability and electrochemical reaction kinetics. Overall, to improve the application performance of conversion-type anode materials in FLBs, researchers are committed to alleviating volume changes and voltage hysteresis through various strategies, including carbon coating, composites with conductive materials, construction of conductive networks, and nano-structuring design, to achieve better electrochemical performance and cycling stability. Table 2 summarizes the flexibility and electrochemical performance of anode materials with different Li^+ storage mechanisms prepared by electrospinning. In summary, electrospinning technology demonstrates significant potential in the fabrication of anode materials with excellent electrical conductivity and good structural stability. By employing core-shell structures, self-supporting flexible electrode designs, and composite strategies, the issues of high volumetric

Table 2. Li^+ storage mechanism, flexibility evaluation and electrochemical properties in LIBs of various anode materials prepared by electrospinning

Materials	Li^+ storage type	Flexibility evaluation	Capacity/current density/cycles	Ref.
N-doped carbon nanofiber-encapsulated Li_3VO_4 nanoparticles	Intercalation-type	-	736.8 mAh g^{-1}/500 mA g^{-1}/500	[82]
Bio-N doped composite carbon nanofibrous mats	Intercalation-type	Foldable	327 mAh g^{-1}/100 mA g^{-1}/300	[83]
Coal-based carbon fibers	Intercalation-type	Flexible, tensible	408.1 mAh g^{-1}/100 mA g^{-1}/200	[84]
Polyacrylonitrile carbon nanofibers	Intercalation-type	-	375.5 mAh g^{-1}/0.2 C/100	[85]
Porous nitrogen-doped carbon nanofiber membranes	Intercalation-type	Flexible	311 mAh g^{-1}/1,000 mA g^{-1}/1,000	[86]
Titania-based nanotubular	Intercalation-type	Flexible	175 mAh g^{-1}/100 mA g^{-1}/80	[87]
$Li_4Ti_5O_{12}/TiO_2$ heterostructured nanorods	Intercalation-type	-	160.3 mAh g^{-1}/1 C/200	[88]
$Na_{0.35}La_{0.55}TiO_3$ embedded in carbon fibers	Intercalation-type	Bendable	217 mAh g^{-1}/200 mA g^{-1}/100	[89]
Co-MOF/MXene composites	Intercalation-type	Foldable	422 mAh g^{-1}/1,000 mA g^{-1}/500	[90]
Hollow copper/carbon nanotubes and rigid $Ti_3C_2T_x$MXene nanosheets	Intercalation-type	Flexible	378.05 mAh g^{-1}/5,000 mA g^{-1}/1,000	[91]
Carbon-coated MXene nanofiber	Intercalation-type	Flexible	over 400 mAh g^{-1}/2,000 mA g^{-1}/1,000	[92]
Nitrogen-doped Sn/C film	Alloy-type	Bendable	429.1 mAh g^{-1}/5,000 mA g^{-1}/1,000	[93]
Porous carbon nanofibers wrapping Sn nanoparticles	Alloy-type	Bendable	610.8 mAh g^{-1}/200 mA g^{-1}/180	[94]
Sn-Cu alloy particles Encapsulated into carbon nanofibers	Alloy-type	Flexible	501.8 mAh g^{-1}/100 mA g^{-1}/100	[95]
Si@C Core-Shell Nanofibers	Alloy-type	Bendable, windable	762.0 mAh g^{-1}/100 mA g^{-1}/100	[97]
Silica@carbon nanofibers	Alloy-type	Bendable	440 mAh g^{-1}/100 mA g^{-1}/200	[98]
$Si@SiO_x$/CNF	Alloy-type	Flexible	1085	[99]
Silicon@silica@carbon nanofiber	Alloy-type	Bendable	903.7 mAh g^{-1}/100 mA g^{-1}/100	[100]
Nitrogen/carbon network connects hollow carbon nanospheres with silicon nanodots	Alloy-type	Bendable	450 mAh g^{-1}/500 mA g^{-1}/200	[101]
Ge-CNFs nanofibers	Alloy-type	-	795.9 mAh g^{-1}/100 mA g^{-1}/100	[102]
Iron compounds/carbon fibers	Conversion-type	Bendable, foldable	255.3 mAh g^{-1}/1,000 mA g^{-1}/650	[103]
γ-Fe_2O_3@carbon nanofiber	Conversion-type	-	820 mAh g^{-1}/0.5 C/250	[104]
Iron/manganese-based compounds/carbon fibers	Conversion-type	Flexible	750.23 mAh g^{-1}/200 mA g^{-1}/250	[105]
Carbon nanofibers impregnated with Fe_3O_4 nanoparticles	Conversion-type	Flexible	823 mAh g^{-1}/0.3 C/4	[106]
Reduced graphene-doped magnetite carbon nanofiber	Conversion-type	Flexible	1126 mAh g^{-1}/1,000 mA g^{-1}/200	[107]
MXene nanofibers confining MnO_xnanoparticles	Conversion-type	Flexible	1098 mAh g^{-1}/2,000 mA g^{-1}/2,000	[108]
Carbon nanopocket-confined Co_3O_4 within mesoporous carbon nanofiber	Conversion-type	Bendable	503 mAh g^{-1}/2,000 mA g^{-1}/1,000	[109]
Sb_2S_3/TiO_2/C nanofiber	Conversion-type	Flexible, foldable, and twistable	261.6 mAh g^{-1}/50 mA g^{-1}/100	[110]
Nickel-coated CNFs with uniform $NiGa_2S_4$ nanosheets	Conversion-type	Bendable, foldable	1349 mAh g^{-1}/62.5 mA g^{-1}/1	[111]
FeP_2/P/C nanofiber	Conversion-type	Flexible	974.3 mAh g^{-1}/5,000 mA g^{-1}/280	[113]
$ZnSnO_3$ microcubes functionalized in-doped carbon nanofibers	Conversion-type	Flexible	582.6 mAh g^{-1}/100 mA g^{-1}/100	[114]

expansion during alloying and poor electrical conductivity of Si-based anode materials can be mitigated, thereby enhancing the electrochemical performance of FLBs.

INTERFACE ENGINEERING AND FULL-CELL CONFIGURATION

Interface issues hold significant research value in FLBs, including the interfaces between active material particles and electrospun polymer matrices or their derived carbon matrices, and between fiber electrodes and electrolytes. In some cases, there is also an interface between fiber-based electrodes and binders and conductive agents. Interface issues are key factors affecting the cyclic stability of fiber-based electrode materials. In the manufacturing of full-cells for FLBs, stable interface structures and strong anchoring effects can prevent slippage and delamination of FLBs under external mechanical stress.

For the interface regulation between active material particles and polymer matrices, titanium (IV) isopropoxide can be used as a coupling agent to enhance the thermal and mechanical properties of Sb_2S_3/TiO_2/C nanofibers[110]. Its negatively charged oxygen atoms can bind with positively charged transition metal ions, while the isopropyl groups also promote strong binding between transition metal ions and linear polymers through entanglement. The use of coupling agents alleviates the issues of structural failure and poor flexibility during thermal treatment in traditional electrospun fiber membranes caused by incompatibility and low adhesion at the interface between polymers and transition metal ions. Even after four times folds, the Sb_2S_3/TiO_2/C nanofiber membrane shows no creases, and the full cell assembled with it as the anode exhibits a high capacity of 261.6 mAh g^{-1} after 100 cycles at 50 mA g^{-1}.

Furthermore, it is worth noting that the structure and chemical composition of the interface between the electrode and electrolyte are key factors affecting the electrochemical performance of fiber-based electrodes. Poor interfacial reactions can lead to the formation of a SEI with high impedance, causing continuous polarization increase. Therefore, the rational design of SEI is crucial for FLBs. SiO_x, due to its large volume changes during charging and discharging, experiences repeated tearing and reorganization of its formed SEI. The continuously growing SEI forms a large impedance at the interface, which is not only detrimental to cycling but also exhibits poor mechanical properties, even leading to powdering and detachment. TiO_2, as an anode material with strong mechanical properties and minimal volume change during Li^+ insertion and extraction, can provide mechanical buffering for SiO_x and enhance interface stability. Tan *et al.* encapsulated large-sized (micrometer-level) SiO_x, which is difficult to encapsulate, into fibers composed of TiO_2 and C through ball milling and surface coating[115]. The composite coating of TiO_2/C provides a stable skeleton and good channels for charge transfer and Li^+ diffusion, significantly enhancing interface stability, thus achieving a high retention rate of 89.5% after 100 cycles at 0.4 A g^{-1}. Similarly, SnO_2, as an anode with large volume changes, can also improve its interface stability by being encapsulated in TiO_2[116].

In addition to addressing SEI stability issues on the electrode side, solid polymer electrolytes (SPE) have become an important component of FLBs due to their high safety, light weight, and excellent flexibility, often playing a significant role in interface stability. PEO, as a widely studied SPE, has ether chains that can serve as pathways for Li^+ conduction. To increase the Li^+ transport capacity of PEO, Gao *et al.* realized an SPE with Poly-m-phenyleneisophthalamide (PMIA) as the skeleton and PEO as the filling polymer through electrospinning and electrostatic spraying[117]. On the one hand, the close interface contact between the two polymers reduces internal defects in the SPE, which is conducive to high-speed and uniform Li^+ conduction. On the other hand, the uniform SPE structure and uniform Li^+ transport enhance the stability of the SPE against lithium metal and cathodes such as NCM and LFP, with lower SEI interface resistance. PVDF-based SPE, as another widely studied SPE, requires the formation of solvation structures with residual solvents such as N-methylpyrrolidone (NMP) or DMF for Li^+ transport, and the decomposition of residual solvents

during cycling may lead to SEI instability. Fang *et al.* induced the release of fluoride ions from lithium salts in PVDF-HFP by introducing $Li_7La_3Zr_2O_{12}$ (LLZO), and the decomposition of more free FSI^- ions formed an inorganic SEI dominated by LiF[118]. The excellent interface structure allows the pouch cell to withstand bending, puncturing, and even cutting.

In the design for full-cells, coaxial electrospinning technology is considered promising as it can change the spinning solution types to alter the spinning materials, thus achieving good anchoring at the interface between polymer electrolytes and electrodes. Wang *et al.* used LFP as the receiving substrate and electrospun SPE on it to achieve the composite of electrodes and electrolytes[119]. To enhance the interface affinity of PVDF-HFP with LFP during electrospinning and improve mechanical properties, Al_2O_3 nanoparticles were mixed with PVDF-HFP, and poly(m-phenylene isophthalamide) (PMIA) was injected into the center of PVDF-HFP/Al_2O_3 nanofibers to form a core-shell structure. The good interface contact between LFP and SPE promotes the transfer of Li^+ and interface stability, achieving a retention rate of 96.6% after 600 cycles at 1 C. In addition to the cathode, the anode (such as graphite) can also be compounded with the separator in a similar way to achieve high interface stability. The special interlocking structure enhances the adhesion strength and interface compatibility between the fiber separator and the graphite anode[120].

In summary, interface issues are crucial for battery performance, affecting the interaction between active material particles and polymer matrices and the contact between fiber electrodes and electrolytes. Excellent interface contact can achieve lower interface impedance and maintain excellent electrochemical performance under mechanical stress such as bending. The comprehensive application of these strategies provides an effective technical path for the development of high-performance, high-stability full-cells for FLBs.

CONCLUSION AND OUTLOOK

With the surge in demand for wearable electronics and medical devices, FLBs have emerged as an innovative solution due to their exceptional adaptability and durability. These batteries not only conform closely to the human body but also adapt to varying shapes and sizes, and withstand continuous bending and twisting, while offering long cycle life and safety. Standardized assessment methods are crucial for the further development of FLBs, ensuring reliable testing of battery flexibility, and this review emphasizes the importance of standardized assessment methods. Electrospinning technology plays a significant role in the manufacturing of FLBs, particularly in the production of fiber materials for the cathodes and anodes. Firstly, electrospinning can alter the physicochemical properties of materials, not only improving the brittleness of inorganic electrode materials but also enabling fast Li^+ conduction through composite with carbon, thereby achieving flexible electrodes with high-rate performance. Secondly, electrospinning facilitates the continuous production of electrodes, which allows for large-scale industrialization and is beneficial for practical applications. Thirdly, electrospinning has unique advantages in the integration of electrode materials with separator materials and the integration of multifunctional devices, enabling the creation of ultra-thin multifunctional electronic devices.

The review highlights the significant progress made in the development of cathode and anode materials through electrospinning. From polyanion-type cathodes to oxide cathodes, and from intercalation-type to alloy-type and conversion-type anodes, electrospinning technology provides solutions to improve the inherent defects of various types of cathode and anode materials, achieving FLBs with high energy density and cycle stability.

FLBs, with their outstanding performance, are expected to become a key force in driving the rapid expansion of the global wearable technology market, providing an ideal solution for modern wearable devices. This review proposes the following prospects for the future development of FLBs:

(1) Optimization of assessment standards and regulatory systems: Establishing a comprehensive assessment and regulatory system is particularly important for the development of FLBs. This requires the development of a complete and standardized set of tests, including their flexibility and electrochemical stability under different conditions. The development of standardized testing instruments and methods is helpful for the assessment of FLBs. In addition, regulatory agencies need to ensure that FLB products meet uniformity standards.

(2) In-depth exploration of electrode material optimization and composite strategies: To achieve higher energy density and longer cycle life, the development of new flexible electrode materials and the optimization of existing electrode materials are important avenues. It is worth noting that some organic electrodes with Li^+ storage sites, such as PIs, not only exhibit high discharge capacity but also have good flexibility. They can be produced on a large scale through methods such as electrospinning, and further exploration of their optimization is warranted. Moreover, the combination of different materials and structural designs can improve the inherent defects of certain electrode materials and control costs. For example, compounding with carbon materials can enhance the conductivity of the electrode and mitigate volume expansion. The composite with porous structures is beneficial for the storage of Li^+ and the alleviation of stress, which is worth further exploration.

(3) Optimization of electrospinning equipment and processes: For electrospinning technology that can achieve large-scale production of fiber-based cathode and anode materials, the optimization of its parameters is crucial for producing fibers with the desired diameter and morphology. Innovations in electrospinning equipment, such as multi-nozzle systems or precise control modules, also help form fibers with specific nanostructures.

(4) Integration with other flexible devices: As an energy supply system, the integration of FLBs with other functional electronic devices is an inevitable trend. Currently, electrospinning has been applied in the fabrication of electronic devices such as triboelectric nanogenerators and electronic skin[121,122]. The method of integrating FLBs with other electronic devices by altering the pre-electrospinning solution is worth further exploration. To achieve comfortable wearable flexible electronic devices, the coordination and integration between FLBs and other technologies, such as integrated design, are worth in-depth exploration, which requires interdisciplinary collaboration.

(5) Enhancement of environmental protection and safety: FLBs must not only meet user demands but also comply with the principles of environmental sustainability. The development of eco-friendly FLBs must consider the entire life cycle, from material extraction to disposal. For example, in electrospinning technology, the selection of sustainable precursors and environmentally friendly solvents is helpful in achieving eco-friendly fiber-based electrode materials. Additionally, advancing FLB safety features, such as flame retardancy and thermal runaway protection, warrants further research and development.

DECLARATIONS

Authors' contributions

Conceptualization, Investigation, and Writing - Original Draft: Li, Z.; Li, M.

Formal Analysis: Li, Z.; Li, M.; He, W.; Fei, B.
Supervision and Writing - Review & Editing: Fei, B.

Availability of data and materials
Not applicable.

Financial support and sponsorship
This work was supported by General Research Fund PolyU152189/21E from the Hong Kong Research Grant Council, and was also supported by The ESG and Sustainable Fashion Hub of Greater Bay Area (1-WZ2H).

Conflicts of interest
All authors declared that there are no conflicts of interest.

Ethical approval and consent to participate
Not applicable.

Consent for publication
Not applicable.

REFERENCES
1. Wearable technology market size, share & trends analysis report by product (eyewear & headwear, wristwear), by application (consumer electronics, healthcare), by region, and segment forecasts, 2025-2030. Available from: https://www.grandviewresearch.com/industry-analysis/wearable-technology-market [Last accessed on 10 Mar 2025].
2. Ahmadabadi V, Shirvanimoghaddam K, Kerr R, Showkath N, Naebe M. Structure-rate performance relationship in Si nanoparticles-carbon nanofiber composite as flexible anode for lithium-ion batteries. *Electrochim. Acta.* **2020**, *330*, 135232. DOI
3. Xu, C.; Fan, Z.; Zhang, M.; et al. A comparative study of the venting gas of lithium-ion batteries during thermal runaway triggered by various methods. *Cell. Rep. Phys. Sci.* **2023**, *4*, 101705. DOI
4. Ke, B.; Cheng, S.; Zhang, C.; et al. Low-temperature flexible integration of all-solid-state thin-film lithium batteries enabled by spin-coating electrode architecture. *Adv. Energy. Mater.* **2024**, *14*, 2303757. DOI
5. Gao, Z.; Zhou, Y.; Zhang, J.; et al. Advanced energy harvesters and energy storage for powering wearable and implantable medical devices. *Adv. Mater.* **2024**, *36*, e2404492. DOI
6. Ye, T.; Wang, J.; Jiao, Y.; et al. A tissue-like soft all-hydrogel battery. *Adv. Mater.* **2022**, *34*, e2105120. DOI
7. Lu, C.; Jiang, H.; Cheng, X.; et al. High-performance fibre battery with polymer gel electrolyte. *Nature* **2024**, *629*, 86-91. DOI
8. Zhao, C.; Wang, R.; Liang, H.; et al. Autonomous self-healing strategy for flexible fiber lithium-ion battery with ultra-high mechanical properties and volumetric energy densities. *Chem. Eng. J.* **2024**, *496*, 154153. DOI
9. Hassan, M. M.; Wang, X.; Bristi, A. A.; Yang, R.; Li, X.; Lu, Q. Composite scaffold of electrospun nano-porous cellulose acetate membrane casted with chitosan for flexible solid-state sodium-ion batteries. *Nano. Energy.* **2024**, *128*, 109971. DOI
10. Wan, X.; Zhao, Y.; Li, Z.; Li, L. Emerging polymeric electrospun fibers: from structural diversity to application in flexible bioelectronics and tissue engineering. *Exploration* **2022**, *2*, 20210029. DOI PubMed PMC
11. Cheng, X.; Liu, Y. T.; Si, Y.; Yu, J.; Ding, B. Direct synthesis of highly stretchable ceramic nanofibrous aerogels via 3D reaction electrospinning. *Nat. Commun.* **2022**, *13*, 2637. DOI PubMed PMC
12. Liu, C.; Liao, Y.; Jiao, W.; et al. High toughness combined with high strength in oxide ceramic nanofibers. *Adv. Mater.* **2023**, *35*, e2304401. DOI
13. Xie, G.; Tan, X.; Shi, Z.; et al. SiO_x based anodes for advanced Li-ion batteries: recent progress and perspectives. *Adv. Funct. Mater.* **2025**, *35*, 2414714. DOI
14. Huang, Q.; Wang, D.; Zheng, Z. Nanocarbon materials toward textile-based electrochemical energy storage devices. In: Nanocarbon Electrochemistry; 2020, pp.123-43. DOI
15. Wu, W.; Liu, M.; Pei, Y.; et al. Unprecedented superhigh-rate and ultrastable anode for high-power battery via cationic disordering. *Adv. Energy. Mater.* **2022**, *12*, 2201130. DOI
16. Huang, Q.; Liu, L.; Wang, D.; Liu, J.; Huang, Z.; Zheng, Z. One-step electrospinning of carbon nanowebs on metallic textiles for

high-capacitance supercapacitor fabrics. *J. Mater. Chem. A.* **2016**, *4*, 6802-8. DOI
17. Chang, J.; Huang, Q.; Gao, Y.; Zheng, Z. Pathways of developing high-energy-density flexible lithium batteries. *Adv. Mater.* **2021**, *33*, e2004419. DOI
18. Zhang, T.; Ju, J.; Zhang, Z.; Su, D.; Wang, Y.; Kang, W. Wearable flexible zinc-ion batteries based on electrospinning technology. *J. Energy. Chem.* **2024**, *98*, 562-87. DOI
19. Li, H.; Qu, R.; Ma, Z.; Zhou, N.; Huang, Q.; Zheng, Z. Permeable and patternable super-stretchable liquid metal fiber for constructing high-integration-density multifunctional electronic fibers. *Adv. Funct. Mater.* **2024**, *34*, 2308120. DOI
20. Ding, Y.; Jiang, J.; Wu, Y.; et al. Porous conductive textiles for wearable electronics. *Chem. Rev.* **2024**, *124*, 1535-648. DOI
21. He, F.; Wang, Y.; Liu, J.; Yao, X. One-dimensional carbon based nanoreactor fabrication by electrospinning for sustainable catalysis. *Exploration* **2023**, *3*, 20220164. DOI PubMed PMC
22. Khurram, T. M.; Ahmed, A.; Rafiq, M.; et al. Chemistry aspects and designing strategies of flexible materials for high-performance flexible lithium-ion batteries. *Chem. Rec.* **2024**, *24*, e202300155. DOI
23. Li, H.; Tang, Z.; Liu, Z.; Zhi, C. Evaluating flexibility and wearability of flexible energy storage devices. *Joule* **2019**, *3*, 613-9. DOI
24. Xiao, G.; Ju, J.; Li, M.; et al. Weavable yarn-shaped supercapacitor in sweat-activated self-charging power textile for wireless sweat biosensing. *Biosens. Bioelectron.* **2023**, *235*, 115389. DOI
25. Shao, G.; Yu, R.; Zhang, X.; et al. Making stretchable hybrid supercapacitors by knitting non-stretchable metal fibers. *Adv. Funct. Mater.* **2020**, *30*, 2003153. DOI
26. Ji, D.; Lin, Y.; Guo, X.; et al. Electrospinning of nanofibres. *Nat. Rev. Methods. Primers.* **2024**, *4*, 278. DOI
27. Dinuwan, G. K. R. S.; Simorangkir, R. B. V. B.; McGuinness, G. B.; et al. The potential of electrospinning to enable the realization of energy-autonomous wearable sensing systems. *ACS. Nano.* **2024**, *18*, 2649-84. DOI PubMed PMC
28. Chen, L.; Mei, S.; Fu, K.; Zhou, J. Spinning the future: the convergence of nanofiber technologies and yarn fabrication. *ACS. Nano.* **2024**, *18*, 15358-86. DOI
29. Huang, Y.; Li, Y.; Zhang, Y.; Yu, H.; Tan, Z. Near-field electrospinning for 2D and 3D structuring: fundamentals, methods, and applications. *Mater. Today. Adv.* **2024**, *21*, 100461. DOI
30. Taylor, G. I.; Van, D. M. D. Electrically driven jets. *Proc. R. Soc. Lond. A.* **1969**, *313*, 453-75. DOI
31. Si, Y.; Shi, S.; Hu, J. Electrospinning and electrospraying synergism: twins-tech collaboration across dimensions. *Matter* **2024**, *7*, 1373-405. DOI
32. Zhang, Z.; Huang, X.; Hong, D.; Ye, P.; Chen, Z.; Xu, Q. Mechanism and experimental investigation on the formation of micro-triangle stepped jet in composite spinning solution. *Polym. Eng. Sci.* **2024**, *64*, 4309-20. DOI
33. Fang, J.; Niu, H.; Wang, H.; Wang, X.; Lin, T. Enhanced mechanical energy harvesting using needleless electrospun poly(vinylidene fluoride) nanofibre webs. *Energy. Environ. Sci.* **2013**, *6*, 2196. DOI
34. Yoo, J.; Kim, D. H.; Pyo, S. G.; Balasingam, S. K. Eletrospinning: improving the performance of 1-D nanofibers used in anodes, cathodes, and separators in lithium-ion batteries. *Int. J. Energy. Res.* **2024**, *2024*, 1847943. DOI
35. Xue, M.; Quan, Z.; Qin, X.; Yu, J.; Li, Y. Impacts of viscosity on bending behavior of the electrospun jet: simulation model and experiment. *Polymer* **2024**, *311*, 127529. DOI
36. Han, Y.; Shi, C.; Cui, F.; Chen, Q.; Tao, Y.; Li, Y. Solution properties and electrospinning of polyacrylamide and ε-polylysine complexes. *Polymer* **2020**, *204*, 122806. DOI
37. Kheilbash, M.; Pirsalami, S.; Malayeri, M. R.; Zebarjad, S. M.; Riazi, M. Use of mixed low/high vapor pressure solvent as a novel solvent design strategy for tuning fiber diameter in electrospun mats. *J. Polym. Res.* **2024**, *31*, 3940. DOI
38. Dong, T.; Arifeen, W. U.; Choi, J.; Yoo, K.; Ko, T. Surface-modified electrospun polyacrylonitrile nano-membrane for a lithium-ion battery separator based on phase separation mechanism. *Chem. Eng. J.* **2020**, *398*, 125646. DOI
39. Asgari, S.; Mohammadi, Z. G.; Badiei, A.; Vasseghian, Y. Zr-UiO-66, ionic liquid ($HMIM^{+}TFSI^{-}$), and electrospun nanofibers (polyacrylonitrile): all in one as a piezo-photocatalyst for degradation of organic dye. *Chem. Eng. J.* **2024**, *487*, 150600. DOI
40. Wang, X.; Zhu, S.; Dong, X.; Huang, H.; Qi, M. Ionic liquid assisted electrospinning synthesis for ultra-uniform Sn@ mesoporous carbon nanofibers as a flexible self-standing anode for lithium ion batteries. *J. Alloys. Compd.* **2021**, *866*, 158984. DOI
41. Souza, R. J.; Soares, F. J. E.; Simões, T. A.; Oliveira, J. E.; Medeiros, E. S. Experimental investigation of solution blow spinning nozzle geometry and processing parameters on fiber morphology. *ACS. Appl. Polym. Mater.* **2024**, *6*, 9735-43. DOI
42. Khan, J.; Khan, A.; Khan, M. Q.; Khan, H. Applications of co-axial electrospinning in the biomedical field. *Next. Mater.* **2024**, *3*, 100138. DOI
43. Kim, B. G.; Kang, D. W.; Park, G.; Park, S. H.; Lee, S.; Choi, J. W. Electrospun Li-confinable hollow carbon fibers for highly stable Li-metal batteries. *Chem. Eng. J.* **2021**, *422*, 130017. DOI
44. Hu, T.; Shen, X.; Peng, L.; et al. Preparation of single-ion conductor solid polymer electrolyte by multi-nozzle electrospinning process for lithium-ion batteries. *J. Phys. Chem. Solids.* **2021**, *158*, 110229. DOI
45. Kılıç, A.; Yıldırım, B.; İçoğlu, H. İ.; Türkoğlu, M.; Topalbekiroğlu, M. Production of continuous nanofiber bundles by multi parallel electrodes in needleless electrospinning. *Mater. Today. Commun.* **2024**, *39*, 109025. DOI
46. Jin, J.; Yeom, S. H.; Lee, H. J.; Choi, C. K.; Lee, S. H. The effect of nozzle spacing on the electric field and fiber size distribution in a multi-nozzle electrospinning system. *J. Appl. Polym. Sci.* **2023**, *140*, e53764. DOI
47. Ding, L.; Li, R.; Gao, Y.; et al. Electrospun nanofibers for fragile artifact conservation. *Compos. Commun.* **2024**, *46*, 101824. DOI
48. Yıldırım, B.; Kılıç, A.; İçoğlu, H. İ.; Türkoğlu, M.; Topalbekiroğlu, M. Continuous nanofiber bundle production using helical

spinnerets with different configurations in needleless electrospinning. *Adv. Eng. Mater.* **2024**, *26*, 2400989. DOI

49. Norzain, N. A.; Lin, W. C. Orientated and diameter-controlled fibrous scaffolds fabricated using the centrifugal electrospinning technique for stimulating the behaviours of fibroblast cells. *J. Ind. Text.* **2022**, *51*, 6728S-52S. DOI
50. Sun, L.; Cai, Y.; Kim, D.; et al. Enhanced properties of solid polymer electrolytes by a bilayer nonwoven PET/nanofiber PVDF substrate for use in all-solid-state lithium metal batteries. *J. Power. Sources.* **2023**, *564*, 232851. DOI
51. Zeng, Z.; Shao, Z.; Shen, R.; et al. Coaxial electrospun Tai chi-inspired lithium-ion battery separator with high performance and fireproofing capacity. *ACS. Appl. Mater. Interfaces.* **2023**, *15*, 44259-67. DOI
52. Yu, Y.; Liu, M.; Chen, Z.; et al. Advances in nonwoven-based separators for lithium-ion batteries. *Adv. Fiber. Mater.* **2023**, *5*, 1827-51. DOI
53. Zhang, S.; Li, Y.; Xu, G.; et al. High-capacity $Li_2Mn_{0.8}Fe_{0.2}SiO_4$/carbon composite nanofiber cathodes for lithium-ion batteries. *J. Power. Sources.* **2012**, *213*, 10-5. DOI
54. Song, H. J.; Kim, J.; Choi, M.; et al. Li_2MnSiO_4 nanorods-embedded carbon nanofibers for lithium-ion battery electrodes. *Electrochim. Acta.* **2015**, *180*, 756-62. DOI
55. Mados, E.; Atar, I.; Gratz, Y.; et al. Polymer-based LFP cathode/current collector microfiber-meshes with bi- and interlayered architectures for Li-ion battery. *J. Power. Sources.* **2024**, *603*, 234397. DOI
56. Akhmetova, K.; Tatykayev, B.; Kalybekkyzy, S.; Sultanov, F.; Bakenov, Z.; Mentbayeva, A. One-step fabrication of all-in-one flexible nanofibrous lithium-ion battery. *J. Energy. Storage.* **2023**, *65*, 107237. DOI
57. Zhijiang, C.; Xingjuan, S.; Yanan, F. Electrochemical properties of electrospun polyindole nanofibers as a polymer electrode for lithium ion secondary battery. *J. Power. Sources.* **2013**, *227*, 53-9. DOI
58. Xiong, Y.; Li, Y.; Hu, Z.; et al. Nonsolvent-induced electrospun fibers with crater-like surface and high-loading polytriphenylamine-derived as a flexible cathode for lithium-ion batteries. *Surf. Interfaces.* **2024**, *46*, 104126. DOI
59. Park, H.; Song, T.; Tripathi, R.; Nazar, L. F.; Paik, U. Li_2MnSiO_4/carbon nanofiber cathodes for Li-ion batteries. *Ionics* **2014**, *20*, 1351-9. DOI
60. Zhang, C.; Liang, Y.; Yao, L.; Qiu, Y. Effect of thermal treatment on the properties of electrospun $LiFePO_4$-carbon nanofiber composite cathode materials for lithium-ion batteries. *J. Alloys. Compd.* **2015**, *627*, 91-100. DOI
61. Liu, J.; Hu, X.; Ran, F.; Wang, K.; Dai, J.; Zhu, X. Electrospinning-assisted construction of 3D $LiFePO_4$@rGO/carbon nanofibers as flexible cathode to boost the rate capabilities of lithium-ion batteries. *Ceram. Int.* **2023**, *49*, 1401-8. DOI
62. Kwon, O. H.; Oh, J. H.; Gu, B.; et al. Porous SnO_2/C nanofiber anodes and $LiFePO_4$/C nanofiber cathodes with a wrinkle structure for stretchable lithium polymer batteries with high electrochemical performance. *Adv. Sci.* **2020**, *7*, 2001358. DOI
63. Hongtong, R.; Thanwisai, P.; Yensano, R.; Nash, J.; Srilomsak, S.; Meethong, N. Core-shell electrospun and doped $LiFePO_4$/FeS/C composite fibers for Li-ion batteries. *J. Alloys. Compd.* **2019**, *804*, 339-47. DOI
64. Chen, W.; Xu, D.; Chen, Y.; et al. In situ electrospinning synthesis of N-doped C nanofibers with uniform embedding of Mn doped $MFe_{1-x}Mn_xPO_4$ (M = Li, Na) as a high performance cathode for lithium/sodium-ion batteries. *Adv. Mater. Inter.* **2020**, *7*, 2000684. DOI
65. Shin, J.; Yang, J.; Sergey, C.; Song, M. S.; Kang, Y. M. Carbon nanofibers heavy laden with $Li_3V_2(PO_4)_3$ particles featuring superb kinetics for high-power lithium ion battery. *Adv. Sci.* **2017**, *4*, 1700128. DOI PubMed PMC
66. Lokeswararao, Y.; Dakshinamurthy, A. C.; Budumuru, A. K.; Sudakar, C. Influence of nano-fibrous and nano-particulate morphology on the rate capability of $Li_3V_2(PO_4)_3$/C Li-ion battery cathode. *Mater. Res. Bull.* **2023**, *166*, 112331. DOI
67. Gavali, D. S.; Abhijitha, V. G.; Nanda, B.; Thapa, R. Origin of high stability, enhanced specific capacity, and low Li diffusion energy in boron doped $Li_3V_2(PO_4)_3$. *J. Energy. Storage.* **2023**, *69*, 107899. DOI
68. Zeng, W.; Xia, F.; Wang, J.; et al. Entropy-increased $LiMn_2O_4$-based positive electrodes for fast-charging lithium metal batteries. *Nat. Commun.* **2024**, *15*, 7371. DOI PubMed PMC
69. Duan, L.; Zhang, X.; Yue, K.; Wu, Y.; Zhuang, J.; Lü, W. Synthesis and electrochemical property of $LiMn_2O_4$ porous hollow nanofiber as cathode for lithium-ion batteries. *Nanoscale. Res. Lett.* **2017**, *12*, 109. DOI PubMed PMC
70. Xu, R.; Zhang, X.; Chamoun, R.; et al. Enhanced rate performance of $LiNi_{0.5}Mn_{1.5}O_4$ fibers synthesized by electrospinning. *Nano. Energy.* **2015**, *15*, 616-24. DOI
71. Kim, N.; Gi, M. K.; Chandio, Z. A.; Park, J.; Cheong, J. Y.; Jung, J. Breaking limits of Li-ion batteries with high-voltage spinel $LiNi_{0.5}Mn_{1.5}O_4$ nanofiber/carbon nanotube composite cathodes. *Korean. J. Chem. Eng.* **2024**, *41*, 1513-20. DOI
72. Mizushima, K.; Jones, P.; Wiseman, P.; Goodenough, J. Li_xCoO_2 (0<x<-1): A new cathode material for batteries of high energy density. *Mater. Res. Bull.* **1980**, *15*, 783-9. DOI
73. Kap, Ö.; Inan, A.; Er, M.; Horzum, N. Li-ion battery cathode performance from the electrospun binary $LiCoO_2$ to ternary $Li_2CoTi_3O_8$. *J. Mater. Sci. Mater. Electron.* **2020**, *31*, 8394-402. DOI
74. Min, J. W.; Yim, C. J.; Im, W. B. Facile synthesis of electrospun $Li_{1.2}Ni_{0.17}Co_{0.17}Mn_{0.5}O_2$ nanofiber and its enhanced high-rate performance for lithium-ion battery applications. *ACS. Appl. Mater. Interfaces.* **2013**, *5*, 7765-9. DOI PubMed
75. Jin, Y.; Zong, X.; Zhang, X.; Jia, Z.; Tan, S.; Xiong, Y. Cathode structural design enabling interconnected ionic/electronic transport channels for high-performance solid-state lithium batteries. *J. Power. Sources.* **2022**, *530*, 231297. DOI
76. Zhao, J.; Kang, T.; Chu, Y.; et al. A polyimide cathode with superior stability and rate capability for lithium-ion batteries. *Nano. Res.* **2019**, *12*, 1355-60. DOI
77. Li, D.; Cheng, H.; Hao, X.; et al. Wood-derived freestanding carbon-based electrode with hierarchical structure for industrial-level

hydrogen production. *Adv. Mater.* **2024**, *36*, e2304917. DOI

78. Cao, Z.; Sang, M.; Chen, S.; et al. In situ constructed (010)-oriented $LiFePO_4$ nanocrystals/carbon nanofiber hybrid network: Facile synthesis of free-standing cathodes for lithium-ion batteries. *Electrochim. Acta.* **2020**, *333*, 135538. DOI
79. Chen, L. L.; Yang, H.; Jing, M. X.; et al. A novel all-fiber-based $LiFePO_4$/$Li_4Ti_5O_{12}$ battery with self-standing nanofiber membrane electrodes. *Beilstein. J. Nanotechnol.* **2019**, *10*, 2229-37. DOI PubMed PMC
80. Peng, Y.; Tan, R.; Ma, J.; Li, Q.; Wang, T.; Duan, X. Electrospun $Li_3V_2(PO_4)_3$ nanocubes/carbon nanofibers as free-standing cathodes for high-performance lithium-ion batteries. *J. Mater. Chem. A.* **2019**, *7*, 14681-8. DOI
81. Jing, M.; Pi, Z.; Zhai, H.; et al. Three-dimensional $Li_3V_2(PO_4)_3$/C nanowire and nanofiber hybrid membrane as a self-standing, binder-free cathode for lithium ion batteries. *RSC. Adv.* **2016**, *6*, 71574-80. DOI
82. Yang, S.; Pei, C.; Zhang, D.; et al. Hierarchical porous N-doped carbon nanofibers with encapsulated Li_3VO_4 nanoparticles for lithium-ion storage. *ACS. Appl. Nano. Mater.* **2024**, *7*, 827-35. DOI
83. Wang, Z.; Kang, K.; Wu, J.; et al. Comparative effects of electrospinning ways for fabricating green, sustainable, flexible, porous, nanofibrous cellulose/chitosan carbon mats as anode materials for lithium-ion batteries. *J. Mater. Res. Technol.* **2021**, *11*, 50-61. DOI
84. Han, X.; Guo, H.; Xing, B.; et al. A facile electrospinning strategy to prepare cost-effective carbon fibers as a self-supporting anode for lithium-ion batteries. *Fuel* **2024**, *373*, 132277. DOI
85. Rao, X.; Lou, Y.; Zhao, J.; et al. Carbon nanofibers derived from carbonization of electrospinning polyacrylonitrile (PAN) as high performance anode material for lithium ion batteries. *J. Porous. Mater.* **2023**, *30*, 403-19. DOI
86. Xu, H.; Hou, X.; Yang, Y.; et al. Flexible and crosslinking electrospun porous carbon nanofiber membranes as freestanding binder-free anodes for lithium-ion batteries. *J. Energy. Storage.* **2024**, *86*, 111281. DOI
87. Charkhesht, V.; Yarar, K. B.; Alkan, G. S.; Yürüm, A. Electrospun nanotubular titania and polymeric interfaces for high energy density Li-ion electrodes. *Energy. Fuels.* **2023**, *37*, 6197-207. DOI PubMed PMC
88. Zhou, Y.; Xiao, S.; Jiang, J.; Wu, R.; Niu, X.; Chen, J. S. In-situ construction of $Li_4Ti_5O_{12}$/rutile TiO_2 heterostructured nanorods for robust and high-power lithium storage. *Nano. Res.* **2023**, *16*, 1513-21. DOI
89. Cao, K.; Zhu, Y.; He, H.; et al. Zero-strain sodium lanthanum titanate perovskite embedded in flexible carbon fibers as a long-span anode for lithium-ion batteries. *ACS. Appl. Mater. Interfaces.* **2024**, *16*, 11421-30. DOI
90. Chen, Y.; Cheng, J.; Wang, A.; et al. The enhanced performance of Li-ion batteries based on Co-MOF/MXene composites. *Inorg. Chem. Commun.* **2024**, *159*, 111793. DOI
91. Liu, J.; Ma, L.; Li, S.; et al. Three-dimensional architecture using hollow Cu/C nanofiber interpenetrated with MXenes for high-rate lithium-ion batteries. *Rare. Met.* **2023**, *42*, 3378-86. DOI
92. Xiao, J.; Jin, Q.; Cang, R.; Gao, H.; Yao, J. Carbon-coated MXene nanofiber as a free-standing electrode for high-performance lithium-ion storage. *Electrochim. Acta.* **2023**, *451*, 142289. DOI
93. Yang, M.; Liu, L.; Yan, H.; et al. Porous nitrogen-doped Sn/C film as free-standing anodes for lithium ion batteries. *Appl. Surf. Sci.* **2021**, *551*, 149246. DOI
94. Zhu, S.; Huang, A.; Wang, Q.; Xu, Y. MOF-derived porous carbon nanofibers wrapping Sn nanoparticles as flexible anodes for lithium/sodium ion batteries. *Nanotechnology* **2021**, *32*, 165401. DOI PubMed
95. Xin, Y.; Mou, H.; Miao, C.; et al. Encapsulating Sn-Cu alloy particles into carbon nanofibers as improved performance anodes for lithium-ion batteries. *J. Alloys. Compd.* **2022**, *922*, 166176. DOI
96. Li, W.; Peng, J.; Li, H.; et al. Encapsulating nanoscale silicon inside carbon fiber as flexible self-supporting anode material for lithium-ion battery. *ACS. Appl. Energy. Mater.* **2021**, *4*, 8529-37. DOI
97. Zeng, L.; Xi, H.; Liu, X.; Zhang, C. Coaxial electrospinning construction Si@C core-shell nanofibers for advanced flexible lithium-ion batteries. *Nanomaterials* **2021**, *11*, 3454. DOI PubMed PMC
98. Sun, N.; Wang, X.; Dong, X.; Huang, H.; Qi, M. PVP-grafted synthesis for uniform electrospinning silica@carbon nanofibers as flexible free-standing anode for Li-ion batteries. *Solid. State. Ion.* **2022**, *374*, 115817. DOI
99. Xian, Z.; Tao, J.; Yu, J.; et al. Si@SiO_x/CNF flexible anode prepared by electrospinning for Li-ion batteries. *Russ. J. Electrochem.* **2023**, *59*, 430-40. DOI
100. Li, X.; Wang, X.; Li, J.; et al. High-performance, flexible, binder-free silicon-carbon anode for lithium storage applications. *Electrochem. Commun.* **2022**, *137*, 107257. DOI
101. Zhu, R.; Wang, Z.; Hu, X.; Liu, X.; Wang, H. Silicon in hollow carbon nanospheres assembled microspheres cross-linked with N-doped carbon fibers toward a binder free, high performance, and flexible anode for lithium-ion batteries. *Adv. Funct. Mater.* **2021**, *31*, 2101487. DOI
102. Zhang, T.; Huang, T.; Li, X.; et al. Ultra-high rapid-charging performance of 1D germanium anode materials for lithium-ion batteries. *J. Alloys. Compd.* **2024**, *976*, 173287. DOI
103. Sheng, X.; Li, T.; Sun, M.; et al. Flexible electrospun iron compounds/carbon fibers: phase transformation and electrochemical properties. *Electrochim. Acta.* **2022**, *407*, 139892. DOI
104. Su, Y.; Fu, B.; Yuan, G.; et al. Three-dimensional mesoporous γ-Fe_2O_3@carbon nanofiber network as high performance anode material for lithium- and sodium-ion batteries. *Nanotechnology* **2020**, *31*, 155401. DOI
105. Xie, F.; Sheng, X.; Ling, Z.; et al. Flexible electrospun iron/manganese-based compounds/carbon fibers: phase transformation and electrochemical properties. *Electrochim. Acta.* **2023**, *470*, 143288. DOI
106. Velásquez, C.; Vásquez, F.; Alvarez-Láinez, M.; Zapata-González, A.; Calderón, J. Carbon nanofibers impregnated with Fe_3O_4

nanoparticles as a flexible and high capacity negative electrode for lithium-ion batteries. *J. Alloys. Compd.* **2021**, *862*, 158045. DOI

107. Rosaiah, P.; Niyitanga, T.; Sambasivam, S.; Kim, H. Graphene based magnetite carbon nanofiber composites as anodes for high-performance Li-ion batteries. *New. J. Chem.* **2022**, *47*, 482-90. DOI
108. Guo, Y.; Zhang, D.; Bai, Z.; et al. MXene nanofibers confining MnO_x nanoparticles: a flexible anode for high-speed lithium ion storage networks. *Dalton. Trans.* **2022**, *51*, 1423-33. DOI
109. Kim, K.; Song, Y.; Ahn, H. Quantum dot-derived carbon nanopocket-confined Co_3O_4 within mesoporous carbon nanofiber for Cu-free anode of flexible Li-ion batteries. *Appl. Surf. Sci.* **2023**, *637*, 157905. DOI
110. Xia, J.; Zhang, X.; Yang, Y.; Wang, X.; Yao, J. Electrospinning fabrication of flexible, foldable, and twistable Sb_2S_3/TiO_2/C nanofiber anode for lithium ion batteries. *Chem. Eng. J.* **2021**, *413*, 127400. DOI
111. Kim, Y.; Samuel, E.; Huh, J.; An, S.; Lee, H.; Yoon, S. S. Carbon-nickel core-shell nanofibers decorated with bimetallic nickel-gallium chalcogenide nanosheets as flexible, binder-free lithium-ion-battery anodes. *Intl. J. Energy. Res.* **2022**, *46*, 21797-811. DOI
112. Zhang, C.; Shen, L.; Shen, J.; et al. Anion-sorbent composite separators for high-rate lithium-ion batteries. *Adv. Mater.* **2019**, *31*, e1808338. DOI
113. Zhan, L.; Song, X.; Deng, W.; et al. Facile approach to prepare FeP_2/P/C nanofiber heterostructure via electrospinning as highly performance self-supporting anode for Li/Na ion batteries. *Electrochim. Acta.* **2022**, *403*, 139682. DOI
114. Li, X.; Guan, G.; Yu, C.; et al. Enhanced electrochemical performances based on $ZnSnO_3$ microcubes functionalized in-doped carbon nanofibers as free-standing anode materials. *Dalton. Trans.* **2023**, *52*, 11187-95. DOI
115. Tan, F.; Guo, H.; Wang, Z.; et al. Electrospinning-enabled SiO@TiO_2/C fibers as anode materials for lithium-ion batteries. *J. Alloys. Compd.* **2021**, *888*, 161635. DOI
116. Mou, H.; Chen, S.; Xiao, W.; et al. Encapsulating homogenous ultra-fine SnO_2/TiO_2 particles into carbon nanofibers through electrospinning as high-performance anodes for lithium-ion batteries. *Ceram. Int.* **2021**, *47*, 19945-54. DOI
117. Gao, L.; Liang, H.; Li, J.; Cheng, B.; Deng, N.; Kang, W. The high-strength and ultra-thin composite electrolyte using one-step electrospinning/electrostatic spraying process for interface control in all-solid-state lithium metal battery. *J. Power. Sources.* **2021**, *515*, 230622. DOI
118. Fang, Z.; Zhao, M.; Peng, Y.; Guan, S. Combining organic plastic salts with a bicontinuous electrospun PVDF-HFP/$Li_7La_3Zr_2O_{12}$ membrane: LiF-rich solid-electrolyte interphase enabling stable solid-state lithium metal batteries. *ACS. Appl. Mater. Interfaces.* **2022**, *14*, 18922-34. DOI
119. Wang, L.; Yan, J.; Zhang, R.; et al. Core-shell pmia@ PVDF-HFP/Al_2O_3 nanofiber mats in situ coaxial electrospun on $LiFePO_4$ electrode as matrices for gel electrolytes. *ACS. Appl. Mater. Interfaces.* **2021**, *13*, 9875-84. DOI
120. Xiao, W.; Cheng, D.; Huang, L.; Song, J.; Yang, Z.; Qiao, Q. An integrated separator/anode assembly based on electrospinning technique for advanced lithium-ion batteries. *Electrochim. Acta.* **2021**, *389*, 138776. DOI
121. Shi, S.; Ming, Y.; Wu, H.; et al. A bionic skin for health management: excellent breathability, in situ sensing, and big data analysis. *Adv. Mater.* **2024**, *36*, e2306435. DOI
122. Chen, Q.; Akram, W.; Cao, Y.; Ge, C.; Lin, T.; Fang, J. Recent progress in the fabrication and processing of triboelectric yarns. *Carbon. Neutralization.* **2023**, *2*, 63-89. DOI